

1 **Trends analysis of PM source contributions and chemical tracers in NE Spain during 2004 - 2014:**

2 **A multi-exponential approach.**

4 *Marco Pandolfi^{1*}, Andrés Alastuey¹, Noemí Pérez¹, Cristina Reche¹, Iria Castro¹, Victor Shatalov² and Xavier Querol¹*

5 ¹ *Institute of Environmental Assessment and Water Research, c/ Jordi-Girona 18-26, 08034 Barcelona, Spain*

6 ² *Meteorological Synthesizing Centre – East, 2nd Roshchinsky proezd, 8/5, 115419 Moscow, Russia*

7 *Corresponding author: *marco.pandolfi@idaea.csic.es*

10 **Abstract**

11 In this work for the first time data from two twin stations (Barcelona, urban background, and Montseny, regional background), located in NE of Spain, were used to study the trends of the concentrations of different chemical species in PM₁₀ and PM_{2.5} along with the trends of the PM₁₀ source contributions from Positive Matrix Factorization (PMF) model. Eleven years of chemical data (2004–2014) were used for this study. Trends of both specie concentrations and source contributions were studied using the Mann-Kendall test for linear trends and a new approach based on multi-exponential fit of the data. Despite the fact that different PM fractions (PM_{2.5}, PM₁₀) showed linear decreasing trends at both stations, the contributions of specific sources of pollutants and of their chemical tracers showed exponential decreasing trends. The different types of trends observed reflected the different effectiveness and/or time of implementation of the measures taken to reduce the concentrations of atmospheric pollutants. Moreover, the trends of the contributions of specific sources such as those related with industrial activities and with primary energy consumption mirrored the effect of the financial crisis in Spain from 2008. The sources that showed statistically significant downward trends at both Barcelona (BCN) and Montseny (MSY) during 2004-2014 were *Secondary sulfate*, *Secondary nitrate*, and *V-Ni bearing* source. The contributions from these sources decreased exponentially during the considered period indicating that the observed reductions were not gradual and consistent over time. Conversely, the trends were less steep at the end of the period compared to the beginning thus likely indicating the attainment of a lower limit. Moreover, statistically significant decreasing trends were observed for the contributions to PM from the *Industrial/Traffic* source at MSY (mixed metallurgy and road traffic) and from the *Industrial* (metallurgy mainly) source at BCN. These sources were clearly linked with anthropogenic activities and the observed decreasing trends confirmed the effectiveness of pollution control measures implemented at EU or regional/local levels. Conversely, at regional level the contributions from sources mostly linked with natural processes such as *Aged Marine* and *Aged Organics* did not show statistically significant trends. The trends observed for the PM₁₀ source contributions well reflected the trends observed for the chemical tracers of these pollutant sources.

35 **1. Introduction**

36 Meeting the air quality (AQ) standards is one of the major environmental objectives to protect people from
37 breathing air with high levels of pollution. Many studies have been published in these last years showing clearly
38 that the concentrations of particulate matter (PM), and other air pollutants such as sulfur dioxide (SO_2) and
39 carbon monoxide (CO), have markedly decreased during the last 15 years in many European Countries (EEA,
40 2013; Barmpadimos et al., 2012; Cusack et al., 2012; Querol et al., 2014; Guerreiro et al., 2014 among others).
41 Cusack et al. (2012) reported the reduction in $\text{PM}_{2.5}$ concentrations observed at regional background (RB)
42 stations in Spain and across Europe, and, in most cases, the observed reduction was gradual and consistent over
43 time implying the success of cleaner anthropogenic activities. Barmpadimos et al. (2012) have also shown that
44 PM_{10} concentrations decreased at a number of urban background (UB) and rural background stations in five
45 European countries. Henschel et al. (2013) reported the dramatic decrease in SO_2 levels in six European cities
46 which reflected the reduction in sulfur content in fuels, as part of EU legislation, coupled with the shift towards
47 the use of cleaner fuels. EEA (2013) also reported general decreases in NO_2 concentrations even if lower
48 compared to PM. However, Henschel et al. (2015) showed that the NO_x concentrations at traffic sites in many
49 EU cities remained unchanged underlining the need of further regulative measures to meet the air quality
50 standards for this pollutant. In fact an important proportion of the European population lives in areas exceeding
51 the AQ standards for the annual limit value of NO_2 , the daily limit value of PM_{10} and the health protection
52 objective of O_3 (EEA, 2013; 2015). PM_{10} and NO_2 are still exceeded mostly in urban areas, and especially at
53 traffic sites (Harrison et al., 2008; Williams and Carslaw, 2011; EEA, 2013; among others). In Spain for example it
54 has been reported that more than 90% of the NO_2 exceedances can be attributed to road traffic emissions
55 (Querol et al., 2012). Guerreiro et al. (2014) furthermore evidenced the notable reduction of ambient air
56 concentration of SO_2 , CO and Pb using data available in Airbase (EEA, 2013) covering 38 European countries.
57 Querol et al. (2014) reported trends for 73 measurement sites across Spain including RB, UB, traffic stations (TS)
58 and Industrial sites (IND). They observed marked downward trends for the concentrations of PM_{10} , $\text{PM}_{2.5}$, CO
59 and SO_2 at most of the RB, UB, TR and IND sites considered. Similarly, Salvador et al. (2012) detected statistically
60 significant downward trends for the concentrations of SO_2 , NO_x , CO and $\text{PM}_{2.5}$ at most of the urban and urban-
61 background monitoring sites in the Madrid metropolitan area during 1999-2008. Cusack et al. (2012) and Querol
62 et al. (2014) have also shown the statistically significant decreasing trends for many trace elements (Pb, Cu, Zn,
63 Mn, Cd, As, Sn, V, Ni, Cr) at regional level in NE Spain since 2002.

64 The observed reduction of air pollutants across Europe is the results of efficient emission abatement strategies
65 as for example those implemented in the Industrial Emission Directives (IPPC Integrated Pollution Prevention
66 and Control and subsequent Industrial Emission Directives 1996/61/EC and 2008/1/EC), the Large Combustion
67 Plants Directive (LCPD; 2001/80/EC), the EURO standards on road traffic emission (1998/69/EC, 2002/80/EC,
68 2007/715/EC), the IMO (International Maritime Organization) directive on sulfur content in fuel and SO_x and
69 NO_x emissions from ships (IMO, 2011; Directive 2005/33/EC). Additionally, the financial crisis, causing mainly a

70 reduction of the primary energy consumption from 2008-2009, contributed to the decrease of the ambient
71 concentration of pollutants observed in Spain (Querol et al., 2014).

72 Moreover, national and regional measures for AQ have been taken in many European Countries. In Spain a
73 national AQ plan was approved in 2011 and updated in 2013 by the Council of Ministers of the Government of
74 Spain. Furthermore, 45 regional and 3 local (city scale) AQ plans have been implemented since 2004 in Spain.
75 These AQ Plans mostly focused on improving AQ at major city centers and specific industrial areas.

76 Thanks to the aforementioned measures there is clear evidence that the concentrations of PM in many
77 European countries have markedly decreased during the last decades. However, in spite of the above policy
78 efforts, a significant proportion of the urban population in Europe lives in areas exceeding the World Health
79 Organisation (WHO) AQ standards for example for $\text{PM}_{2.5}$, PM_{10} and O_3 (EEA, 2013, 2015).

80 The analysis of the trends of the concentration of air pollutants helps in evaluating the effectiveness of specific
81 AQ measures depending on the pollutant considered. Examining data over time also makes it possible to predict
82 future frequencies and/or rates of occurrence making future projections. For the abovementioned reasons, it is
83 especially attractive the feasibility of studying the trends of the contributions to PM mass from specific
84 pollutant sources along with the trends of the chemical tracers of these sources.

85 For what we are concerned in the majority of studies dealing with trend analysis linear fits were applied by
86 using Mann-Kendall or Theil-Sen methods (Theil, 1950; Sen, 1968), the latter being available for example in the
87 Openair software (Carslaw, 2012; Carslaw and Ropkins, 2012). However, a linear fit of data does not always
88 properly represent the observed trends. As we will show, different abatement strategies and periods of
89 implementation may change from one pollutant to another thus leading to different trends for different
90 pollutants even over the same period. Thus, non-linear fit of the data may be at times strongly recommended.

91 The main aim of this work was to study the trends of PM_{10} source contributions and of specific chemical species
92 in both PM_{10} and $\text{PM}_{2.5}$ using both the consensus methodology (Mann-Kendall) and the non-linear approach.
93 The data of Spanish national emissions and energy consumption were also evaluated to interpret the observed
94 trends. Understanding past trends may be relevant for devising new strategies for air pollution abatement. PM
95 chemical speciated data collected from 2004 to 2014 at regional (Montseny; NE Spain) and urban (Barcelona,
96 NE Spain) sites were used with this aim. The Positive Matrix Factorization (PMF) model was used to apportion
97 ambient PM_{10} concentrations into pollutant sources. The PMF model, as other Receptor Models (RM), is widely
98 used being a powerful tool to help policy makers to design more targeted approaches to protecting public
99 health. Thus, the novelty of this study lies mainly in a) the opportunity to study the trends of pollutant source
100 contributions from PMF model at two twin stations representative of the urban and regional environments in
101 the Western Mediterranean, and, b) in the use of a novel non-linear approach for trend studies.

103 **2. Measurement sites and Methodology**

104 **2.1 Measurement sites**

105 The Montseny measurement station (MSY, 41°46'45.63" N, 02°21'28.92" E, 720 m a.s.l.) is a regional
106 background site in NE of Spain located in a regional natural park about 50 km to the NNE of the city of
107 Barcelona (BCN) and 25 km from the Mediterranean coast (Figure 1). This site is representative of the typical
108 regional background conditions of the Western Mediterranean Basin (WMB) characterized by severe pollution
109 episodes affecting not only the coastal sites closest to the emission sources, but also the more elevated rural
110 and remote areas land inwards (i.e. Pérez et al., 2008; Pey et al., 2010; Pandolfi et al., 2011; 2014). This station
111 is part of the ACTRIS (www.actris.net) and GAW (www.wmo.int/gaw) networks, of the EMEP Program
112 (<http://www.emep.int/>) and of the measuring network of the Government of Catalonia.

113 The Barcelona measurement station (BCN, 41°23'24.01" N, 02°06'58.06" E, 68 m a.s.l.) is an urban background
114 measurement site influenced by vehicular emissions from one of the main avenues of the city (Diagonal
115 Avenue) located at a distance of around 300 m (cf. Fig. 1). The BCN measurement site is part of the Air Quality
116 measuring network of the Government of Catalonia. The Metropolitan Area of Barcelona (BMA), with nearly 4.5
117 million inhabitants, covers an 8 km wide strip between the Mediterranean Sea and the coastal mountain range.
118 Several industrial zones, power plants, and highways are located in the area, making this region one of the most
119 polluted in the WMB (i.e. Querol et al., 2008; Amato et al., 2009; Pandolfi et al., 2012; 2013; 2014). At BCN the
120 location of the measuring station changed in 2009 when it was moved by around 500 m (cf. Fig. 1). The effect of
121 this change on PM measurements performed at BCN will discuss later.

122

123 **2.2 Real-time and gravimetric PM measurements**

124 Real-time PM concentrations were continuously measured at 1h resolution by optical particle counters (OPC)
125 using GRIMM spectrometers (GRIMM 180 at MSY, and GRIMM 1107, 1129 and 180 at BCN). Hourly PM
126 concentrations were corrected by comparison with 24h gravimetric mass measurements of PM_x (Alastuey et al.,
127 2011).

128 For gravimetric measurements 24h PM_x samples were collected at both stations every 3-4 days on 150 mm
129 quartz micro-fiber filters (Pallflex QAT and Whatman) with a high-volume (Hi-Vol) samplers (DIGITEL DH80
130 and/or MCV CAV-A/MSb at 30 m³h⁻¹). The mass of PM₁₀ and PM_{2.5} samples collected on filters was determined
131 using the EN 12341 and the EN14907 gravimetric procedures, respectively.

132

133

134

135 **2.2.1 PM chemical speciated data**

136 Once the gravimetric mass was determined from filters, the samples were analyzed with different techniques
137 including acidic digestion ($\frac{1}{2}$ of each filter; $\text{HNO}_3:\text{HF}:\text{HClO}_4$), water extraction of soluble anions ($\frac{1}{4}$ of each filter),
138 and thermal-optical analysis (1.5 cm^2 sections). Inductively Coupled Atomic Emission Spectrometry, ICP-AES,
139 (IRIS Advantage TJA Solutions, THERMO) was used for the determination of the major elements (Al, Ca, Fe, K,
140 Na, Mg, S, Ti, P), and Inductively Coupled Plasma Mass Spectrometry, ICP-MS, (X Series II, THERMO) for the
141 trace elements (Li, Ti, V, Cr, Mn, Co, Ni, Cu, Zn, As, Se, Rb, Sr, Cd, Sn, Sb, Ba, rare earths, Pb, Bi, Th, U). Ionic
142 Chromatography was used for the concentrations of NO_3^- , SO_4^{2-} and Cl^- , whereas NH_4^+ was determined using a
143 specific electrode MODEL 710 A+, THERMO Orion. The levels of OC and EC were determined by a thermal-
144 optical carbon analyzer (SUNSET), using protocol EUSAAR_2 (Cavalli et al., 2010). Other analytical details may be
145 found in Querol et al. (2008).

146 Following the above procedures a total of 1093 PM_{10} and 794 $\text{PM}_{2.5}$ filters were collected and analysed at MSY
147 during the period 2004-2014. At BCN the collected filters were 1037 and 1063 in PM_{10} and $\text{PM}_{2.5}$, respectively.

148

149 **2.3 Positive Matrix Factorization (PMF) model.**

150 The PMF model (PMFv5.0, EPA) was applied to the collected daily PM_{10} speciated data for source identification
151 and apportionment at both sites. Detailed information about the PMF model can be found in literature (Paatero
152 and Tapper 1994; Paatero 1997; Paatero and Hopke 2003; Paatero et al. 2005). The PMF model is a factor
153 analytical tool reducing the dimension of the input matrix in a limited number of factors (or sources) and it is
154 based on the weighted least-squares method. Thus, most important in PMF applications is the estimation of
155 uncertainties of the chemical species included in the input matrix. In the present study, individual uncertainties
156 and detection limits were calculated as in Escrig et al. (2009) and Amato et al. (2009). Thus, both the analytical
157 uncertainties and the standard deviations of species concentrations in the blank filters were considered in the
158 uncertainties calculations. The signal-to-noise ratio (S/N) was estimated starting from the calculated
159 uncertainties and used as a criteria ($S/N > 2$) for selecting the species used within the PMF model. In order to
160 avoid any bias in the PMF results, the data matrix was uncensored (Paatero 2004). The PMF was run in robust
161 mode (Paatero 1997), and rotational ambiguity was handled by means of the F_{PEAK} parameter (Paatero et al.
162 2005). The optimal number of sources was selected by inspecting the variation of the objective function Q
163 (defined as the ratio between residuals and errors in each data value) with varying number of sources (i.e.
164 Paatero et al., 2002) and by studying the physical meaningfulness of the calculated factors.

165

166

167

168 **2.4 Mann-Kendall (MK) fit**

169 The purpose of the Mann-Kendall (MK) test (Mann 1945, Kendall 1975, Gilbert 1987) is to statistically assess if
170 there is a monotonic upward or downward trend of the variable of interest with time. A monotonic upward
171 (downward) trend means that the variable consistently increases (decreases) through time. The Mann-Kendall
172 test tests the null hypothesis H_0 of no trend, i.e. the observations are randomly ordered in time, against the
173 alternative hypothesis, H_1 , where there is an increasing or decreasing monotonic trend. The main advantage of
174 the Mann-Kendall test is that data need not conform to any particular distribution and missing data are allowed.
175 To estimate the slope of the trend the Sen's method was used (Salmi et al. 2002).

176

177 **2.5 Multi-exponential (ME) fit**

178 A program aiming at studying trends by means of multi-exponential fit of the data was developed within the
179 *The Task Force on Measurements and Modelling* (TFMM) by the *Meteorological Synthesizing Centre – East*
180 (MSC-E; <http://www.msceast.org/>) group (Shatalov et al., 2015). The TFMM together with the *Task Force on*
181 *Emission Inventories and Projections* (TFEIP), the *Task Force on Integrated Assessment Modelling* (TFIAM), and
182 *Task Force on Hemispheric Transport of Air Pollution* (TFHTAP) provide a fora for discussion and scientific
183 exchange in support of the EMEP (*European Monitoring and Evaluation Programme*; <http://www.emep.int/>)
184 work plan which is a scientifically based and policy driven programme under the *Convention on Long-range*
185 *Transboundary Air Pollution* (CLRTAP; http://www.unece.org/env/lrtap/lrtap_h1.html) to promote the
186 international co-operation and to solve transboundary air pollution problems. The TFMM was established in
187 2000 to evaluate measurements and modeling and to further develop working methods and tools. In this
188 contest, five EMEP Centers are undertaking efforts in support of the EMEP work plan, namely the *MSC-E*, the
189 *Centre on Emission Inventories and Projections* (CEIP; <http://www.ceip.at/>), the *Chemical Coordinating Centre*
190 (CCC; <http://www.nilu.no/projects/ccc/>), the *Meteorological Synthesizing Centre – West* (MSC-W;
191 http://emep.int/mscw/index_mscw.html), and the *Centre for Integrated Assessment Modelling* (CIAM;
192 <http://www.iiasa.ac.at/~rains/ciam.html>). In 2014 the TFMM initiated a dedicated exercise to assess the efficiency of CLRTAP air pollution mitigation strategies over the past 20 years evaluating the benefit of its main
193 policy instruments. Within this exercise a software was made available by EMEP/MSC-E Center aiming at
194 studying non-linear trends. Annual, monthly and daily resolution data can be analyzed with the help of this
195 program. Since in this paper we will apply the program to annual averages of specie concentrations and source
196 contributions, we restrict the description of the multi-exponential approximations for this case. In particular,
197 seasonal variations are not included into consideration. The basic equations solved by the program for this
198 particular case (annual averages) are reported below:

199

201
$$C_t = a_1 \cdot \exp\left(-\frac{t}{\tau_1}\right) + a_2 \cdot \exp\left(-\frac{t}{\tau_2}\right) + \dots + a_n \cdot \exp\left(-\frac{t}{\tau_n}\right) + \omega_t \quad (1)$$

202

203 Where, C_t are the values of the considered time series, with $t = 1, \dots, N$, N being the length of the series (years),
 204 τ_n are the characteristic times of the considered exponential, a_n are constants and ω_t are the residue values. In
 205 the case of single exponential decay ($n=1$) the characteristic time τ is the time at which the pollutant
 206 concentration is reduced to $1/e$ ($= 0.3678$) times its initial value. The main difference between linear and
 207 exponential fit is that in the latter case the trend is not gradual and constant over time. For an exponential
 208 trend the absolute [$\mu\text{g}/\text{m}^3$] reduction per year decreases with time being the highest at the beginning of the
 209 period. Conversely, for a linear fit the absolute reduction is constant over time. For an exponential fit, the lower
 210 the characteristic time τ the more rapidly the considered quantity vanishes. Deviations from single exponential
 211 fit can be taken into account introducing more exponential terms. In this work for example two exponential
 212 terms were sometime used. In this case two characteristic times are calculated by the software. If the decrease
 213 of the considered quantity is very sharp at the beginning of the period (more than single exponential) than both
 214 τ_1 and τ_2 are positive. Conversely, one exponential term with negative τ takes into account for possible increase
 215 of the quantity at the end of the period. Both τ_n and a_n are calculated by the program by means of the least
 216 square method minimizing the residue ω and the statistically significance of the exponential fit is provided by
 217 means of the p-value. The number of exponential terms that should be included into the approximation can be
 218 evaluated using F-statistics (i.e. Smith, 2002). For example, the F-statistics for the evaluation of the statistical
 219 significance of the second term in equation (1) for $n = 2$ can be calculated as:

220

221
$$F = \frac{(SS_1 - SS_2)}{2 \cdot s} \quad (2)$$

222

223 where SS_1 and SS_2 are sums of squares of residual component for approximations with one and two exponential
 224 terms, respectively, and s is the estimate of standard deviation of residual component. This statistics follows
 225 approximately the Fisher distribution with 2 and $N - 2$ degrees of freedom. Second exponential is considered to
 226 be significant if F exceeds the corresponding threshold value at the chosen significance level.

227 The following parameters can be calculated from equation (1):

228 - Total Reduction (TR):
$$TR = \frac{(C_{beg} - C_{end})}{C_{beg}} = 1 - \frac{C_{end}}{C_{beg}} \quad (3)$$

229 - Annual reduction for year i :
$$R_i = \frac{\Delta C_i}{C_i} = 1 - \frac{C_{i+1}}{C_i} \quad (4)$$

230 - Average annual reduction:
$$R_{av} = 1 - \left(\frac{C_{end}}{C_{beg}} \right)^{\frac{1}{N-1}} \quad (5)$$

231 Where C_{beg} and C_{end} are the first and the last points, respectively, of the exponential fit. The formula for the
 232 calculation of the average annual reduction takes into account that the ratio C_{i+1} / C_i is a multiplicative quantity,
 233 so that geometrical mean of ratios should be used. The relative contribution of residues (Residual Component:

234 RC) is calculated as the standard deviation of the ratios between the residue values of the fit ω_t (cf. Eq. 1) and
235 the main component of the fit.

236 The MSC-E also proposed a statistic which measures the deviation of the obtained trend from the linear one
237 (Non-Linearity parameter: NL). A trend is defined as linear if the NL parameter is lower than 10%, indicating a
238 small difference between ME and MK fits (Shatalov et al., 2015). In the following, the reported trends were
239 analysed using the MK test for $NL<10\%$ and the ME test for $NL>10\%$. More detailed description of the multi-
240 exponential approach is available in the TFMM wiki and in the MSC-E Technical report 2015 (Shatalov et al.,
241 2015).

242

243 **3. Results**

244 Results are presented and discussed in the following order: In Section 3.1, we compare the trends at both
245 stations of PM_x concentrations from optical counters (OPC; annual data coverage around 90%) and from 24h
246 gravimetric samples (filters; annual data coverage around 20-30%). This comparison will demonstrate the
247 feasibility of studying trends of chemical species concentrations from filters despite the relatively low annual
248 data coverage. In Section 3.2, we compare the magnitude of the trend of $PM_{2.5}$ concentrations at MSY during
249 2004-2014 (period selected for this study) with the magnitude of trends calculated at the same station over
250 different periods, namely 2002-2010 (the period used in Cusack et al., 2012) and 2002-2014 (representing the
251 largest period of gravimetric $PM_{2.5}$ measurements available at MSY station at the time of writing). This
252 comparison was performed in order to study the differences in the trends over short periods (9 yr to 13 yr). The
253 gravimetric concentrations of $PM_{2.5}$ measured at MSY were used with this aim. Then (Section 3.3), we present
254 and discuss the trends at both stations of chemical species from filters in both PM_{10} and $PM_{2.5}$. In the Section 4.0
255 we discuss the sources of pollutants identified by PMF model in PM_{10} at both sites. Finally, we present and
256 discuss the trends of PM_{10} source contributions at BCN and MSY (Section 4.1) providing possible explanations
257 for the observed trends. Conclusions are reported in Section 5.

258

259 **3.1 Trends of PM: Comparison between gravimetric and real-time optical measurements**

260 Annual data coverage is an important factor to take into account in order to study trends of a given parameter.
261 The gravimetric PM measurements, from which chemical speciated data are obtained, are typically performed
262 with rather low frequency over one year. In our case the annual data coverage of gravimetric measurements
263 was around 20-30% at both Barcelona and Montseny. In this section we compare the trends of PM
264 concentrations from gravimetric and real-time optical measurements (Table 1). Given that the trends of the
265 considered PM_x fractions were linear at both sites ($NL<10\%$), only results from MK test were reported in Table
266 1. However, we will show later (Section 4.1) that the contributions from specific PM_{10} pollutant sources, mainly

267 those related with anthropogenic activities, showed non-linear (i.e. exponential) decreasing trends thus
268 mirroring the different effectiveness of the mitigation strategies depending on the source of pollutants
269 considered.

270 As reported in Table 1, statistically significant decreasing trends were observed for the considered PM size
271 fractions at BCN (-2.20 $\mu\text{gm}^{-3}/\text{yr}$ with $p<0.001$ for PM_{10} and -1.55 $\mu\text{gm}^{-3}/\text{yr}$ with $p<0.01$ for $\text{PM}_{2.5}$ from OPC
272 measurements), whereas at Montseny only the $\text{PM}_{2.5}$ fraction showed a little significant decreasing trend (-0.26
273 $\mu\text{gm}^{-3}/\text{yr}$; $p<0.1$ from OPC measurements). Total reductions (TR) ranged between 50.4% (OPC PM_{10} at BCN) to
274 7.8% (OPC PM_{10} at MSY) and residual component (RC) was lower than 18% reflecting the goodness of the linear
275 (MK) fit used. It must be noted that the higher p-values, magnitude of the trends and TR observed at BCN
276 compared to MSY was likely due to the change of the measuring station in 2009 in BCN (cf. Fig. 1). Based on the
277 comparison between simultaneous PM_x chemical speciated data collected at both BCN measurement sites
278 during 1 month (not shown) we concluded that after 2009 the BCN measuring site was less affected by mineral
279 matter and, to a lesser extent, by road traffic emissions both being important sources of PM in Barcelona. In
280 Figure 1 we highlighted the proximity of the BCN measuring station before 2009 to an unpaved parking and
281 different construction works. The effect of the change of the station in BCN in 2009 on PM_{10} gravimetric
282 measurements was reported in Supporting Information (Figure SI-1). However, despite the change of the
283 station, the comparison between BCN and MSY for specific chemical species and pollutant sources not linked
284 with mineral matter and road traffic emissions was possible.

285 Table 1 shows that the p-values calculated using gravimetric and OPC measurements were the same despite the
286 different annual data coverage. The differences in the magnitude of the trends were 22% and 24% between
287 gravimetric and OPC PM_{10} and $\text{PM}_{2.5}$ measurements, respectively, at BCN and 24% and 21%, respectively, at
288 MSY. Relative differences of total reductions (TR) ranged between 24% between gravimetric and OPC PM_{10}
289 measurements at MSY and 15% for PM_{10} at BCN. Thus, despite the different data coverage the magnitude of the
290 trends and TR calculated from OPC and gravimetric measurements were rather similar. Other PM mass fractions
291 (PM_{1-10} and $\text{PM}_{2.5-10}$) and PM ratios ($\text{PM}_1/\text{PM}_{10}$ and $\text{PM}_{2.5}/\text{PM}_{10}$) at MSY showed non-statistically significant
292 trends.

293

294 **3.2 Trends of PM: Comparison among different periods**

295 In this study we used the period 2004-2014 for trends analysis given that gravimetric $\text{PM}_{2.5}$ measurements at
296 BCN were available since 2004. Conversely, at MSY $\text{PM}_{2.5}$ gravimetric measurements started in 2002. Figure 2
297 shows the trends of $\text{PM}_{2.5}$ concentrations at MSY calculated using the MK test for the three different periods.
298 ME test was not used here given that the observed trends were linear ($\text{NL}<10\%$). The period 2002-2010 was the
299 period considered in the paper from Cusack et al. (2012) presenting the trends of $\text{PM}_{2.5}$ gravimetric mass and
300 chemical species at MSY. The period 2002-2014 is the largest period with $\text{PM}_{2.5}$ filter measurements available at

301 the time of writing. The trend observed at MSY for the PM_{2.5} fraction during 2004-2014 confirmed what already
302 observed by Cusack et al. (2012) at the same station for the period 2002 – 2010. In Cusack et al. (2012) the MK
303 test provided a decreasing trend of around -0.66 $\mu\text{gm}^{-3}/\text{yr}$ at 0.01 significance level (TR = 35%). During the
304 periods 2004 – 2014 and 2002 – 2014 decreasing trends of -0.33 $\mu\text{gm}^{-3}/\text{yr}$ ($p<0.1$; TR = 26%) and -0.37 $\mu\text{gm}^{-3}/\text{yr}$
305 ($p<0.05$; TR = 31%), respectively, were observed. Thus, a statistically significant trend for PM_{2.5} mass at regional
306 level can be observed even considering different periods thus confirming the effectiveness of mitigation
307 measures together with the effect of the economic crisis in Spain from 2008. However, it should be noted that
308 the statistical significance of the trends observed for the larger periods was lower compared to Cusack et al.
309 (2012). The difference observed in the magnitude of the trends during 2004-2014 compared to the results
310 provided by Cusack et al. (2012) was mainly due to the increase of PM_{2.5} mass concentration in 2012 (cf. Figure
311 2). Chemical PM_{2.5} speciated data revealed that this increase was partly driven by organic matter showing a
312 mean annual concentration in 2012 higher by around 20% compared to the 2004-2014 average.

313

314 **3.3 Trends of chemical species**

315 The trends of the annual mean concentrations of chemical species at BCN and MSY are reported in Table 2 (for
316 PM₁₀) and Table 3 (for PM_{2.5}). Figure 3 (for BCN) and Figure 4 (for MSY) show the trends of chemical species in
317 PM₁₀. In Tables 2 and 3 and Figures 3 and 4 only the species having statistically significant trends were reported.

318 As already noted we assume that the change of the station in BCN in 2009 affected the trends of the
319 concentrations of OC, EC, Cu, Sn, Sb and Zn (mainly traffic tracers), Al₂O₃, Ca, Mg, Ti, Rb, Sr (crustal elements
320 related with both natural and anthropogenic sources) and Fe (traffic and crustal tracer). These chemical species
321 at BCN were removed from Tables 2 and 3 and from Figure 3.

322 Other species measured in BCN were not affected by the change of the station. These are SO₄²⁻, NH₄⁺, V, Ni
323 (related with heavy oil combustion in the study area according to source apportionment results, cf. Par. 4), Pb,
324 Cd, and As (related with industrial/metallurgy activities), Na and Cl (sea spray), and NO₃⁻. Although nitrate
325 particles in Barcelona were mainly from traffic, the concentrations of these particles were not strongly affected
326 by the change of the station due to their secondary origin. The MSY station will be considered as reference
327 station given that no location change occurred at this monitoring site during the study period.

328 Statistically significant exponential trends ($p < 0.01$ or 0.001) were mainly observed for the industrial tracers
329 (Pb, Cd, As) in both PM₁₀ and PM_{2.5}. For these elements TR was high and around 50-80% in PM₁₀ and 67-81% in
330 PM_{2.5}. The RCs were lower than 20% thus suggesting the goodness of the exponential fits used to study the
331 trends of these species. Exponential fits were on average needed indicating that the trends were not gradual
332 and consistent over time and that the effectiveness of the control measures for these pollutants was stronger at
333 the beginning of the period under study (2004-2009 approximately) compared to the end of the period (Figs. 3
334 and 4). This is also evident by comparing the linear MK fit (dashed black line) with the ME fit (red line) in Figs. 3

335 and 4. In PM₁₀ the magnitudes of the trends ranged between -0.00222 $\mu\text{gm}^{-3}/\text{yr}$ (Pb; p<0.001) to -3.10E-5 $\mu\text{gm}^{-3}/\text{yr}$ (Cd; p<0.001) at BCN and from -0.00031 $\mu\text{gm}^{-3}/\text{yr}$ (Pb; p<0.01) to -1.12E-5 $\mu\text{gm}^{-3}/\text{yr}$ (Cd; p<0.01) at MSY. In
336 PM_{2.5} the magnitude of the trends were similar and ranged between -0.00163 $\mu\text{gm}^{-3}/\text{yr}$ (Pb; p<0.001) and
337 -3.11E-5 $\mu\text{gm}^{-3}/\text{yr}$ (Cd; p<0.001) at BCN and between -0.00049 $\mu\text{gm}^{-3}/\text{yr}$ (Pb; p<0.001) and -1.35E-5 $\mu\text{gm}^{-3}/\text{yr}$
338 (Cd; p<0.001) at MSY. Similar magnitude of the trends for these species in both PM fractions at both sites
339 confirmed the common origin of these elements and the impact at regional scale of industrial sources. For Pb
340 and Cd the characteristic time (τ) of the exponential trends was similar at both sites, whereas for As it was
341 higher due to the slightly less intense exponential downward trend observed for As compared to Cd and Pb.
342 Note that the PMF analysis (cf. Section 4) revealed that the concentrations of As were explained by multiple
343 sources (especially at BCN) whereas the *Industrial/metallurgy* source alone explained more than around 70% of
344 Pb and Cd concentrations (not shown). The implementation of the IPPC Directive in 2008 in Spain is the most
345 probable cause for this downward trend. The decrease observed for Pb, Cd and As may be also attributed to a
346 decrease in the emissions from industrial production (smelters, Querol et al., 2007) at a regional scale around
347 Barcelona.

349 The concentrations of V and Ni in Barcelona in both PM₁₀ and PM_{2.5} fractions showed very similar exponential
350 decreasing trends. Similar characteristic times (around 10-11 yr), TR (around 59-63%) and RC (15-17%) in both
351 fractions suggested the common and mainly fine origin of these two elements. At MSY, V and Ni showed linear
352 trends likely because of the higher distance of the MSY station to the sources of V and Ni (shipping and, before
353 2008, energy production) compared to BCN. Note also that the NL parameter for BCN V and Ni was around 10-
354 12%, indicating that in this case the exponential fit did not differ very much from the linear one. Total reduction
355 for V and Ni at MSY was around 59-64% and 42-43%, respectively, and RCs were lower than 24%.

356 Sn and Cu in PM₁₀ at MSY showed very similar behavior decreasing linearly with time with TR around 36-39%
357 and RC around 16-20%. Decreasing rates of -3.65E-5 $\mu\text{gm}^{-3}/\text{yr}$ (p<0.05) and -0.00014 $\mu\text{gm}^{-3}/\text{yr}$ (p<0.05) were
358 observed in PM₁₀ for Sn and Cu, respectively. In PM_{2.5}, the concentrations of Sn and Cu decreased markedly
359 compared to PM₁₀ at the rate of -0.00084 $\mu\text{gm}^{-3}/\text{yr}$ (p<0.001) and -0.00026 $\mu\text{gm}^{-3}/\text{yr}$ (p<0.01), respectively. This
360 difference could be explained by possible sources of coarser Sn and Cu which reduced the magnitude of the
361 trends in PM₁₀ mass fraction. Sb showed marked decreasing trends in both PM mass fractions compared to Sn
362 and Cu with TR around 62-70%. The magnitude of the trend for Sb was similar in both fractions and around
363 -3.57 ÷ -3.86E-5 $\mu\text{gm}^{-3}/\text{yr}$. The concentrations of Sb were better fitted with exponential curves (SE with p<0.01
364 in PM₁₀ and DE with p<0.01 in PM_{2.5}). The DE fit for Sb in PM_{2.5} had one positive and one negative characteristic
365 time, the latter needed to explain the slight increase in Sb concentrations at the end of the considered period.
366 The marked decreasing trend observed for Sb compared to other traffic tracers could be explained by a
367 progressive reduction of Sb contained in the vehicle brakes. Cr did not show a statistically significant trend in
368 both PM fractions.

369 Sulfate (SO_4^{2-}) and ammonium (NH_4^+) particles concentrations showed very similar behavior in $\text{PM}_{2.5}$ and PM_{10}
370 size fractions due to their fine nature. In BCN the magnitude of the trends were $-0.37868 \mu\text{gm}^{-3}/\text{yr}$ ($p<0.001$)
371 and $-0.11095 \mu\text{gm}^{-3}/\text{yr}$ ($p<0.001$) for SO_4^{2-} and NH_4^+ , respectively, in PM_{10} and $-0.32778 \mu\text{gm}^{-3}/\text{yr}$ ($p<0.001$) and
372 $-0.12701 \mu\text{gm}^{-3}/\text{yr}$ ($p<0.001$), respectively, in $\text{PM}_{2.5}$. The trends were SE with very similar characteristic times
373 (9.64-9.81 yr in PM_{10} and 9.69-10.53 yr in $\text{PM}_{2.5}$), TR (64-65% in PM_{10} and 61-64% in $\text{PM}_{2.5}$) and RC (12-14% in
374 PM_{10} and 9-15% in $\text{PM}_{2.5}$). At MSY the magnitude of the trends of SO_4^{2-} and NH_4^+ and their statistically
375 significance were lower compared to BCN in both fractions. Moreover, at MSY the trends were linear for SO_4^{2-} in
376 both fractions (as for V and Ni). These differences could be explained by the distance of MSY to direct specific
377 sources of sulfate, such as shipping, compared to BCN, thus slightly reducing the magnitude and the statistically
378 significance of the trend of SO_4^{2-} at regional level. It is also interesting to note the similitude between the
379 characteristic times of the exponential fits for V and Ni and SO_4^{2-} in both PM fractions at BCN suggesting the
380 main common origin of these chemical species. Possible reasons for the observed reduction in the
381 concentrations of ambient sulfate in and around Barcelona will be discussed later.

382 Fine NO_3^- (Table 3) showed statistically significant SE trends similar at both sites with $p<0.001$, TR around 73-
383 82%, RC around 16-21% and characteristic times around 5.8-7.6 yr. In PM_{10} the TR were lower and around 54-
384 64% and the fits were linear at MSY and SE at BCN. The SE fit in PM_{10} at BCN provided a characteristic time
385 around 9.8 yr which was higher compared to the τ obtained for the fine mode (7.6 yr) thus indicating that fine
386 NO_3^- had a more pronounced downward trend compared to $\text{PM}_{10} \text{NO}_3^-$.

387 For the mineral species (Al_2O_3 , Ca, Fe) linear (with the exception of Al_2O_3 in $\text{PM}_{2.5}$ which was SE) and statistically
388 significant decreasing trends were detected at MSY. On average the TR was higher in the fine fraction, ranging
389 from 50% for Ca to 66% for Al_2O_3 , compared to PM_{10} (6-38% cf. Table 2). Downward decreasing trend for crustal
390 material in $\text{PM}_{2.5}$ at MSY was also reported by Cusack et al. (2012) for the period 2002 – 2010 and by Querol et
391 al. (2014) for the period 2001 – 2012. These trends were probably driven by weather conditions associated with
392 negative NAO index (iNAO) that could be the cause for this slight reduction observed in crustal material. Pey et
393 al. (2013) found a correlation between iNAO (calculated between June and September) and the contribution of
394 Saharan dust to PM_{10} mass in NE of Spain and showed that the more negative is the iNAO the lower is the dust
395 contribution to PM. The iNAO was unusually negative during the period 2008 – 2012
396 (<http://www.cpc.ncep.noaa.gov/products/precip/CWlink/pna/norm.nao.monthly.b5001.current.ascii>) thus
397 likely contributing to explain the observed trends of crustal elements. Moreover, negative NAO can favour the
398 presence of fronts that can sweep the Iberian Peninsula from West to East causing stronger winds and less
399 stagnant conditions thus favouring the dispersion of pollutants. In addition, as suggested by Cusack et al (2012),
400 it could also be hypothesised that some part of the crustal material measured at MSY is a product of the
401 construction industry. The construction industry in Spain has been especially affected by the current economic
402 recession and crustal material produced by this industry may have contributed to the crustal load in $\text{PM}_{2.5}$. For
403 example the number of home construction works in Barcelona during 2008 – 2014 (from the beginning of the
404 economic crisis; mean number of works = 1281) reduced by around 75% compared to the period 2000 – 2007;

405 mean number of works = 5187) (<http://www.bcn.cat/estadistica/castella/dades/timm/construccio/index.htm>).
406 The fact that the total reduction calculated for mineral elements reported in Tables 2 and 3 was higher in PM_{2.5}
407 compared to PM₁₀ could corroborate the hypothesis of an anthropogenic contribution to the mineral matter
408 measured at MSY.

409 Finally, Na concentrations showed linear decreasing trends at both sites, with the exception of PM₁₀ Na at MSY.
410 Other species at MSY such as OC and EC did not show statistically significant trends. Consider that the
411 concentrations of EC at MSY are very low and around at 0.2-0.3 µg/m³ as annual mean. Both anthropogenic
412 activity and biomass burning were expected to contribute to this chemical specie. Concerning OC the lack of
413 trend was probably due to the contribution from biogenic sources to the concentration of this specie at regional
414 level.

415

416 **4. PMF source profiles and contributions**

417 Eight and seven sources were detected at BCN and MSY, respectively, in PM₁₀ from PMF model. The absolute
418 and relative contributions of these sources to the measured PM₁₀ mass were reported in Figure 5 whereas the
419 chemical profiles of the detected sources were reported in Supporting Information (Figure SI-2).

420 Some sources were common at both BCN and MSY. These are: *Secondary Sulfate* (secondary inorganic source
421 traced by SO₄²⁻ and NH₄⁺ and contributing 3.95 µg/m³ (23.7%) and 4.67 µg/m³ (13.7%) at MSY and BCN,
422 respectively), *Secondary nitrate* (secondary inorganic source traced by NO₃⁻ and NH₄⁺ and contributing 1.31
423 µg/m³ (7.9%) and 4.45 µg/m³ (13.1%) at MSY and BCN, respectively), *V-Ni bearing* source (traced mainly by V, Ni
424 and SO₄²⁻ it represents the direct emissions from heavy oil combustion and contributed 0.71 µg/m³ (4.3%) and
425 3.32 µg/m³ (9.8%) at MSY and BCN, respectively), *Mineral* (traced by typical crustal elements such as Al, Ca, Ti,
426 Rb, Sr and contributing 2.70 µg/m³ (16.2%) and 4.61 µg/m³ (13.6%) at MSY and BCN, respectively), *Aged marine*
427 (traced by Na and Cl mainly with contributions from SO₄²⁻ and NO₃⁻ and contributing 1.76 µg/m³ (10.6%) and
428 5.73 µg/m³ (16.9%) at MSY and BCN, respectively). Sources detected at MSY but not at BCN were:
429 *Industrial/Traffic* source (traced by EC, OC, Cr, Cu, Zn, As, Cd, Sn, Sb and Pb) which included contributions from
430 anthropogenic sources such as road traffic and metallurgic industries and contributed 1.43 µg/m³ (8.6%) and
431 *Aged organics* (traced mainly by OC and EC) with maxima in summer indicating mainly a biogenic origin and
432 contributing 3.78 µg/m³ (22.7%). The ratio OC:EC in the *Industrial/Traffic* and *Aged organic* source profiles at
433 MSY were 4.2 and 11.7, respectively, thus indicating a strong influence of aged particles in the latter source with
434 the former source being more fresh. The statistic of the OC:EC ratio based on chemical data at MSY is reported
435 in Supporting Information (Figure SI-3). Mean and median values of OC:EC ratio at MSY were 9.1 and 7.8,
436 respectively.

437 Finally, some sources were detected at BCN but not at MSY: *traffic* (traced mainly by C_{nm}, Cr, Cu, Sb and Fe)
438 contributing 5.14 µg/m³ (15.1%), *road/work resuspension* (traced by both crustal elements, mainly Ca, and

439 traffic tracers such as Sb, Cu and Sn) contributing $4.25 \mu\text{g}/\text{m}^3$ (12.5%) and *Industrial/metallurgy* (traced by Pb,
440 Cd, As and Zn) contributing $0.96 \mu\text{g}/\text{m}^3$ (2.8%).

441 A sensitivity study was performed in order to better interpret the PMF sources at BCN. In fact, for the period
442 2007 – 2014 separate OC and EC measurements were available and a PMF was performed over this period. The
443 comparison between the PMF source contributions obtained using the period 2007-2014 (separate OC and EC
444 measurements) and the whole period (2004-2014; C_{nm} (non-mineral carbon) available) is reported in Supporting
445 Information (Figure SI-4). As reported in Figure SI-4 the relative differences in source contributions ranged
446 between -3% (*Mineral* source) to +20% (*Industrial* source) and R^2 ranged between 0.894 to 0.997 thus
447 confirming the correct interpretation of the 2004-2014 PMF sources where C_{nm} was used. The OC:EC ratio in the
448 *Traffic* source from 2007-2014 PMF was 1.70 (cf. Figure SI-5) whereas the mean and median OC:EC ratio from
449 chemistry data were 2.5 and 2.3, respectively, thus being in agreement with the contribution of fresh particles
450 from *Traffic* source at BCN.

451

452 **4.1 Trends of annual PM_{10} source contributions**

453 Figures 6 and 7 and Table 4 show the results from MK or ME test applied to the annual averages of PM_{10} source
454 contributions at BCN and MSY. As already noted we cannot study trends for *Traffic*, *Road/work resuspension*
455 and *Mineral* source contributions at BCN because of the change of the station location in 2009. The
456 contributions that showed statistically significant downward trends at both stations were from *Secondary*
457 *sulfate*, *Secondary nitrate*, and *V-Ni bearing* sources ($p<0.001$ or $p<0.01$). Moreover, statistically significant
458 decreasing trends were observed for the *Industrial/Traffic* ($p<0.01$) and *Mineral* ($p<0.1$) source contributions at
459 MSY and for the *Industrial/metallurgy* source contribution ($p<0.001$) at BCN. These sources were mostly linked
460 with anthropogenic activities and the observed decreasing trends confirmed the effectiveness of pollution
461 control measures together with the possible effect of the economic crisis in Spain from 2008. Conversely, the
462 contributions from sources mostly linked with natural processes such as *Aged Marine* (at both BCN and MSY)
463 and *Aged Organic* (at MSY) did not show statistically significant trends.

464 The trends of the *Secondary sulfate* source contributions were DE and SE at BCN and MSY, respectively, thus
465 indicating that the decrease over time of this source contribution was not gradual and monotonic. Overall the
466 observed decreasing trends at both stations may be attributed to the legislation that came into force in 2007-
467 2008 in Spain (the EC Directive on Large Combustion Plants) which resulted in the application of flue gas
468 desulfurization (FGD) systems in a number of large facilities. Figure 8 shows the sharp decreases after 2007
469 observed for the national SO_2 and NO_x emissions mostly from power generation (MAGRAMA, 2013; Querol et
470 al., 2014). In BCN the two characteristic times (one low and the other high, cf. Table 4) of the DE fit indicated a
471 strong decrease of the *Secondary sulfate* source contribution at the beginning of the period. This decrease was
472 sharper compared to MSY where SE fit was used. This difference was mostly due to the ban of heavy oils and

473 petroleum coke for power generation around Barcelona from 2007. The effects of this AQ Regional Plan were
474 likely more visible in BCN compared to MSY thus explaining the two different exponential fits used. Overall, for
475 the *Secondary sulfate* source contributions the TRs were rather high around 53% at MSY and 67% at BCN with
476 RC ranging from 16% (BCN) to 21% (MSY). The fact that the trend of the *Secondary sulfate* source contribution
477 was exponential likely suggested the attainment of a lower limit and indicated a limited scope for further
478 reduction of SO₂ emissions in our region. In fact, it has been estimated that the maximum in EU will be a further
479 20% reduction through measures in industry, residential and commercial heating and reduced agricultural
480 waste burning (UNECE, 2016). Conversely, in Eastern European countries the scope for reduction is much
481 greater and around 60% (UNECE, 2016).

482 The trends of the *Secondary nitrate* source contributions were SE at both stations with very similar τ (8.96 yr –
483 8.59 yr), TR (67-69 %) and RC (13-17%). The decrease observed for the contribution from the *Secondary Nitrate*
484 source was related to the reduction in ambient NO_x concentrations (Figures 8 and 9). Figure 9 shows the levels
485 of tropospheric NO₂ column from 2005 to 2014 in South Europe from NASA NO₂ OMI level3 plotted using the
486 Giovanni online data system (Acker and Leptoukh, 2007). In Spain it can be observed a general decrease of the
487 concentrations of columnar NO₂ at regional level. Overall, the implementation of European directives affecting
488 industrial and power generation emissions as well as the increase of the proportion of energy produced from
489 renewable sources (cf. Figure 10 for Spain), among others, produced a significant reduction of SO₂ and NO_x
490 emissions. Around Barcelona the observed decreases were also attributed to the decrease of NO_x emissions
491 mainly from the five power generation plants around the city. Moreover, the implementation of the regional
492 AQ Plan for SCRT (continuously regenerating PM traps with selective catalytic reduction for NO₂) and the
493 hybridization and shift to natural gas engines of the Barcelona's bus fleet may have had an influence in the
494 observed reductions.

495 The decreasing trends ($p<0.01$) of the *V-Ni bearing* source contributions were SE and L at BCN and MSY,
496 respectively, reflecting the trends observed at both stations for the concentrations of V and Ni (cf. Table 2). At
497 BCN the characteristic times (τ) were very similar to the characteristic times calculated for PM₁₀ V and Ni (cf.
498 Table 2) which were the main tracers of this source. TRs were around 61% at BCN and 64% at MSY and RCs were
499 similar (19-25 %). The observed decrease in the *V-Ni bearing* source contribution was mainly attributed to the
500 ban of the use of heavy oils and petroleum coke for power generation in Spain from 2008.

501 The *Industrial/Metallurgy* source contribution at BCN decreased exponentially (SE) at the rate of -0.10 $\mu\text{gm}^{-3}/\text{yr}$
502 ($p<0.001$) reflecting the SE decreasing trends observed for the main tracers of this pollutant source (Pb, Cd and
503 As; cf. Table 2). The decrease of industrial emissions was mainly attributed to the implementation of IPPC
504 (Integrated Pollution Prevention and Control) Directives. Moreover, the observed decrease may be attributed to
505 a decrease in the emissions from industrial production (smelters, Querol et al., 2007) at a regional scale around
506 Barcelona. Also, the financial crisis, whose impact on industrial production and use of fuels is evident since
507 October 2008 also contributed to the observed trend. TR and RC for the *Industrial* source contributions at BCN

508 were 65% and 16%, respectively. As for the contributions from *Secondary sulfate* and *nitrate* sources, the
509 exponential trend observed for the *Industrial/Metallurgy* source contribution suggested the attainment of a
510 lower limit. As evidenced in Fig. 6 the contribution from this source from 2010 was quite low and rather
511 constant.

512 The contribution of the *Industrial/Traffic* source at MSY showed similar magnitude of the trend (-0.11 $\mu\text{gm}^{-3}/\text{yr}$)
513 with p<0.01) compared to the BCN *Industrial/Metallurgy* contribution being both sources traced mostly by the
514 same industrial tracers. However, this source at MSY was also traced by traffic tracers (i.e. Cu and Sn) which
515 decreased linearly with time (cf. Table 2), thus likely explaining the linear trend observed for the contribution of
516 this source at MSY. TR and RC were 56% and 13%, respectively, similar to those calculated for *Industrial* source
517 contribution at BCN.

518 Finally, the *Mineral* source contribution at MSY showed linear little significant decreasing trend (p<0.1) in
519 agreement with what observed at the same station by Cusack et al. (2012). As already noted in Section 3.3, this
520 negative trend could be due to both a possible decrease of the emissions of finer anthropogenic mineral species
521 from specific sources such as cement and concrete production and construction works and unusual weather
522 conditions reducing Saharan dust contribution to PM and resuspension of dust.

523 In order to further interpret the observed trends, annual data on the annual National Energy Consumption
524 (NECo) from different energy sources (MINETUR, 2013) were also evaluated (Figure 10). Overall, the primary
525 energy consumption in Spain (NECo statistical data for Spain-MINETUR, 2013) increased from 2004 to 2007 and
526 decreased from 2007 with marked decrease in 2009. Since 2009, the energy consumption indicator remained
527 rather low and constant until 2012 when an additional decrease in 2013 and 2014 was observed. Oil
528 consumption was fairly constant during 2004–2007 showing an important decrease during 2008–2014. This
529 trend was probably governed by the fuel consumption for traffic road. Coal consumption remained constantly
530 high from 2004 to 2007 whereas, as for the emissions of SO₂ (Fig. 8), a sharp decrease occurred from 2007.
531 However, in the period 2011-2014 there was an important increase of coal consumption leading to an average
532 consumption similar to the year 2008. However, the implementation of FGD systems contributed to maintain
533 SO₂ at low concentrations, even in the coal production regions in Spain (cf. Querol et al., 2014). The
534 hydroelectric generation was rather specular to coal consumption. For example, the increase in 2010 of
535 hydroelectric consumption, due to high rainfall rate, mirrored the decrease in the coal consumption observed
536 the same year. Finally, renewable energy consumption increased by 440% from 2004 to 2014, with a gradual
537 growth in the NECo.

538

539 **5.0 Conclusions**

540 PM chemical speciated data collected at two twin stations in NE of Spain (Barcelona: urban background station
541 and Montseny: regional background station) during 2004 – 2014 were used to study the trends of the

542 contributions of pollutant sources from PMF model and of their chemical tracers. Despite the fact the trends of
543 different PM fractions ($PM_{2.5}$ and PM_{10}) were linear during the period under study, the trends of specific
544 chemical elements and source contributions were exponential demonstrating the different effectiveness and/or
545 time of implementation of the different mitigation strategies. Statistically significant exponential trends ($p <$
546 0.01 or 0.001) were mainly observed for the industrial tracers (Pb, Cd, As) in both PM_{10} and $PM_{2.5}$ and at both
547 sites. The concentrations of V and Ni showed exponential trends in BCN and linear trends at MSY likely because
548 of the higher distance of the MSY station to the sources of V and Ni (shipping and, before 2008, energy
549 production) compared to BCN. Traffic tracers at MSY (Sn, Cu) showed very similar linear decreasing trends with
550 higher magnitude of the trends in the fine ($PM_{2.5}$) fractions compared to PM_{10} likely because of possible sources
551 of coarser Sn and Cu reducing the magnitude of the trends in the PM_{10} mass fraction. The concentrations of Sb
552 at MSY showed marked exponential decreasing trend compared to other traffic tracers (Cu and Sn) which could
553 be explained by a possible progressive reduction of Sb content in vehicle brakes. Secondary inorganic aerosols
554 (SO_4^{2-} , NO_3^- and NH_4^+) also showed marked decreasing trends (both linear and exponential) in both fractions and
555 at both sites. However, in general the magnitude of the trends for these species and their statistical significance
556 were higher at BCN compared to MSY.

557 The PM_{10} source contributions that showed statistically significant downward trends at both Barcelona (BCN);
558 UB) and Montseny (MSY; RB) were from *Secondary sulfate*, *Secondary nitrate*, and *V-Ni bearing* sources. For
559 these source contributions the decreasing trends were exponential indicating that the trends were not gradual
560 and consistent over time and that the effectiveness of the control measures for these pollutants was stronger at
561 the beginning of the period under study (2004-2009 approximately) compared to the end of the period
562 considered. Statistically significant decreasing trends were observed for the contributions from *Industrial/Traffic*
563 and *Mineral* sources at MSY and from the *Industrial/metallurgy* source at BCN. These sources were mostly
564 linked with anthropogenic activities and the observed decreasing trends confirmed the effectiveness of
565 pollution control measures implemented at EU or regional/local levels. The economic crisis which started in
566 2008 in Spain also contributed to the observed trends. Conversely, the contributions from sources mostly linked
567 with natural processes such as *Aged Marine* (at both BCN and MSY) and *Aged Organic* (at MSY) did not show
568 statistically significant trends. The general trends observed for the calculated PMF source contributions well
569 reflected the trends observed for the chemical tracers of these pollutant sources. The decrease in the
570 *Secondary sulfate* source contribution was mainly attributed to the EC Directive on Large Combustion Plants
571 implemented in Spain from 2008, resulting in the application of fuels gas desulfurization (FGD) systems in a
572 number of large facilities. Moreover, according to the 2008 Regional AQ Plan, the use of heavy oils and
573 petroleum coke for power generation was forbidden around Barcelona from 2008 in favour of natural gas. As a
574 consequence, a decrease of the contributions from the V-Ni bearing source at both sites was also observed. The
575 decrease observed for the contribution of the *Secondary Nitrate* source was mainly due to the reduction in
576 ambient NO_x concentrations. In Spain a general decrease of the concentrations of NO_2 at regional level was
577 observed and it was mainly related with the lower energy consumption related with the financial crisis. The

578 decrease of nitrates concentrations and *Secondary nitrate* source contributions around Barcelona was also
579 attributed to the decrease of NO_x emissions from the five power generation plants around the city. Moreover, a
580 Regional AQ Plan implementing the SCRT (continuously regenerating PM traps with selective catalytic reduction
581 for NO₂) and the hybridization and shift to natural gas engines of the Barcelona's bus fleet may have had also an
582 influence in NO_x ambient concentrations. The *Industrial/Metallurgy* source contribution at BCN decreased
583 exponentially reflecting the exponential trends observed for the main tracers of this pollutant source (Pb, Cd
584 and As). The implementation of IPPC (Integrated Pollution Prevention and Control) Directives together with a
585 decrease in the emissions from industrial production (smelters) at a regional scale around Barcelona explained
586 the observed trends. Overall, the magnitude of the decreasing trends of the contributions of the pollutant
587 sources were higher at BCN compared to MSY likely because of the proximity of the BCN measurement site to
588 anthropogenic pollutant sources compared to the MSY site. The results presented in this work clearly confirm
589 the beneficial effect of the AQ measures taken in recent years in Europe. However, the WHO limit values of
590 specific pollutants, PM₁₀ and PM_{2.5} among these, are still exceeded especially at urban level and industrial
591 hotspots. To meet the WHO guide levels important actions are still required for the next decade and the
592 interpretation of past air quality trends may yield relevant outcomes for planning further cost-effective actions.
593 We would like to highlight that a non-linear approach to trend studies is very attractive given that some air
594 pollutants reported in this work showed not gradual-with-time reductions. Conversely, for specific pollutant
595 source-contribution/concentration in our region, the decreasing trends were less steep at the end of the period
596 compared to the beginning thus likely indicating the attainment of a lower limit. This was the case for example
597 for the *Secondary sulfate* source contribution decreasing exponentially from 2004 to 2014 thus likely indicating
598 a limited scope for further reduction of SO₂ emissions in our region.

599

600 **Acknowledgments.**

601 This work was supported by the MINECO (Spanish Ministry of Economy and Competitiveness), the MAGRAMA
602 (Spanish Ministry of Agriculture, Food and Environment), the Generalitat de Catalunya (AGAUR 2014 SGR33 and
603 the DGQA) and FEDER funds under the PRISMA project (CGL2012-39623- C02/00). The research leading to these
604 results has received funding from the European Union's Horizon 2020 research and innovation programme
605 under grant agreement No 654109 and previously from the European Union Seventh Framework Programme
606 (FP7/2007-2013) under grant agreement nº 262254. Marco Pandolfi is funded by a Ramón y Cajal Fellowship
607 (RYC-2013-14036) awarded by the Spanish Ministry of Economy and Competitiveness. NO₂ map analyses and
608 visualizations used in this paper were produced with the Giovanni online data system, developed and
609 maintained by the NASA GES DISC. The authors would like to express their gratitude to D. C. Carslaw and K.
610 Ropkins for providing the Openair software used in this paper (Carslaw and Ropkins, 2012; Carslaw, 2012).

611

612

613 **Bibliography**

- 614 Acker, J. G. and Leptoukh, G.: *Online Analysis Enhances Use of NASA Earth Science Data*, Eos, Trans. AGU, 88, 2,
615 14-17, 2007.
- 616 Alastuey, A., Minguillón, M.C., Pérez, N., Querol, X., Viana, M. and de Leeuw, F.: *PM10 Measurement Methods
617 and Correction Factors: 2009 Status Report*, ETC/ACM Technical Paper 2011/21, 2011.
- 618 Amato, F., M. Pandolfi, A. Escrig, X. Querol, A. Alastuey, J. Pey, N. Perez, P.K. Hopke, *Quantifying road dust
619 resuspension in urban environment by Multilinear Engine: A comparison with PMF2*, Atmos. Environ., 43 - 17,
620 pp. 2770 - 2780. 06/2009, 2009.
- 621 Barmpadimos, I., Keller, J., Oderbolz, D., Hueglin, C., Prevot, A.S.H.: *One decade of parallel fine (PM_{2.5}) and
622 coarse (PM₁₀-PM_{2.5}) particulate matter measurements in Europe: trends and variability*, Atmos. Chem. Phys., 12,
623 3189–3203, <http://dx.doi.org/10.5194/acp-12-3189-2012>, 2012
- 624 Carslaw, D.C., *The OpenAir manual — open-source tools for analysing air pollution data*, Manual for version 0.5-
625 16, King's College, London, 2012.
- 626 Carslaw, D.C., Ropkins, K.: *OpenAir — an R package for air quality data analysis*, Environ. Model Softw., 27–28,
627 52–61, 2012
- 628 Cavalli, F., Viana, M., Yttri, K. E., Genberg, J., and Putaud, J.-P.: Toward a standardised thermal-optical protocol
629 for measuring atmospheric organic and elemental carbon: the EUSAAR protocol, Atmos. Meas. Tech., 3, 79-89,
630 doi:10.5194/amt-3-79-2010, 2010.
- 631 Cusack, M., Alastuey, A., Perez, N., Pey, J., Querol, X.: *Trends of particulate matter (PM_{2.5}) and chemical
632 composition at a regional background site in the Western Mediterranean over the last nine years (2002–2010)*,
633 Atmos. Chem. Phys., 12, 8341–8357 <http://dx.doi.org/10.5194/acp-12-8341-2012>, 2012.
- 634 EEA: European Environmental Agency Air quality in Europe — 2013 report, EEA report 9/2013, Copenhagen,
635 1725-9177, [107 pp. <http://www.eea.europa.eu/publications/air-quality-in-europe-2013>], 2013.
- 636 EEA: European Environmental Agency Air quality in Europe — 2015 report, *Many Europeans still exposed to
637 harmful air pollution. Air pollution is the single largest environmental health risk in Europe*, EEA report 11/2015,
638 Copenhagen, 1-7, [<http://www.eea.europa.eu/media/newsreleases/many-europeans-still-exposed-to-air-pollution-2015>], 2015.
- 640 Escrig, A., Monfort, E., Celades, I., Querol, X., Amato, F., Minguillon, M. C., and Hopke, P. K.: Application of
641 optimally scaled target factor analysis for assessing source contribution of ambient PM10, J. Air Waste
642 Manage., 59(11), 1296–1307, 2009.
- 643 Gilbert, R.O.: *Statistical Methods for Environmental Pollution Monitoring*, Wiley, NY, 1987.

- 644 Guerreiro, C., Leeuw, F. de, Foltescu, V., Horálek, J., & European Environment Agency: *Air quality in Europe 2014*
645 report, Luxembourg: Publications Office.
646 <http://bookshop.europa.eu/uri?target=EUB:NOTICE:THAL14005:EN:HTML>, 2014
- 647 Harrison, R.M., Stedman, J., Derwent, D.: *New directions: why are PM10 concentrations in Europe not falling?*,
648 Atmos. Environ., 42, 603–606, 2008.
- 649 Henschel, S., Querol, X., Atkinson, R., Pandolfi, M., Zeka, A., Le Tertre, A., Analitis, A., Katsouyanni, K., Chanel,
650 O., Pascal, M., Bouland, C., Haluza, D., Medina, S., Goodman, P.G.: *Ambient air SO₂ patterns in 6 European*
651 *cities*, Atmos. Environ., 79, 236 - 247. 11/2013, 2013.
- 652 Henschel, S., Le Tertre, A., Atkinson, R.W., Querol, X., Pandolfi, M., Zeka, A., Haluza, D., Antonis, A., Katsouyanni,
653 K., Bouland, C., Pascal, M., Medina, S., Goodman, P.G.: *Trends of nitrogen oxides in ambient air in nine European*
654 *cities between 1999 and 2010*, Atmos. Environ., 117, 234 - 241. 09/2015, 2015.
- 655 Kendall, M.G.: Rank Correlation Methods, 4th edition, Charles Griffin, London, 1975.
- 656 MAGRAMA. *Inventario Nacional de Emisiones de Contaminantes a la Atmósfera*. Ministerio de Agricultura,
657 Alimentación y Medio Ambiente del Gobierno de España. <http://www.magrama.gob.es/ca/calidad-y-evaluacion-ambiental/temas/sistemaespanol-de-inventario-sei-/>, 2013.
- 659 Mann, H.B.: Non-parametric tests against trend, *Econometrica* 13:163-171, 1945.
- 660 MINETUR. Ministerio de Industria, Energía y Turismo. Gobierno de España: energy statistics and balances.
661 <http://www.minetur.gob.es/energia/balances/Balances/Paginas/CoyunturaTrimestral.aspx>, 2013.
- 662 Paatero, P. and Tapper, U.: *Positive Matrix Factorization: a non negative factor model with optimal utilization of error estimates of data values*, *Environmetrics*, 5, 111–126, 1994.
- 664 Paatero, P.: *Least squares formulation of robust non-negative factor analysis*, *Chemometr. Intell. Lab.*, 37, 23–35, 1997.
- 666 Paatero, P., Hopke, P. K., Song, X., and Ramadan, Z.: *Understanding and controlling rotations in factor analytic models*, *Chemometr. Intell. Lab.*, 60(1–2), 253–264, 2002.
- 668 Paatero, P. and Hopke, P. K.: *Discarding or downweighting high noise variables in factor analytic models*, *Anal. Chim. Acta*, 490, 277–289, doi:10.1016/s0003-2670(02)01643-4, 2003.
- 670 Paatero P.: User's guide for positive matrix factorization programs PMF2 and PMF3, Part1: tutorial. University of
671 Helsinki, Helsinki, Finland, 2004.
- 672
- 673 Paatero, P., Hopke, P. K., Begum, B. A., and Biswas, S. K.: *A graphical diagnostic method for assessing the*

- 674 rotation in factor analytical models of atmospheric pollution, Atmos. Environ., 39, 193–201,
675 doi:10.1016/j.atmosenv.2004.08.018, 2005.
- 676 Pandolfi, M., Cusack, M., Alastuey, a. and Querol, X.: Variability of aerosol optical properties in the Western
677 Mediterranean Basin, Atmos. Chem. Phys., 11(15), 8189–8203, doi:10.5194/acp-11-8189-2011, 2011.
- 678 Pandolfi, M., F. Amato, C. Reche, A. Alastuey, R. P. Otjes, M. J. Blom, X. Querol, *Summer ammonia*
679 *measurements in a densely populated Mediterranean city*, Atmos. Chem. Phys., 12, pp. 7557 - 7575. 08/2012,
680 2012.
- 681 Pandolfi, M., G. Martucci, X. Querol, A. Alastuey, F. Wilsenack, S. Frey, C.D. O'Dowd, M. Dall'Osto, *Continuous*
682 *atmospheric boundary layer observations in the coastal urban area of Barcelona during SAPUSS*, Atmos. Chem.
683 Phys., 13 - 9, pp. 4983 - 4996. 05/2013, 2013.
- 684 Pandolfi, M., Querol, X., Alastuey, A., Jimenez, J. L., Jorba, O., Day, D., Ortega, A., Cubison, M. J., Comerón, A.,
685 Sicard, M., Mohr, C., Prévôt, A. S. H., Minguillón, M. C., Pey, J., Baldasano, J. M., Burkhardt, J. F., Seco, R.,
686 Peñuelas, J., van Drooge, B. L., Artiñano, B., Di Marco, C., Nemitz, E., Schallhart, S., Metzger, A., Hansel, A.,
687 Lorente, J., Ng, S., Jayne, J. and Szidat, S.: Effects of sources and meteorology on particulate matter in the
688 Western Mediterranean Basin: An overview of the DAURE campaign, J. Geophys. Res. Atmos., 119(8), 4978–
689 5010, doi:10.1002/2013JD021079, 2014.
- 690 Pérez, N., Pey, J., Castillo, S., Viana, M., Alastuey, A. and Querol, X.: Interpretation of the variability of levels of
691 regional background aerosols in the Western Mediterranean, Sci. Total Environ., 407(1), 527–540,
692 doi:10.1016/j.scitotenv.2008.09.006, 2008.
- 693 Pey, J., Pérez, N., Querol, X., Alastuey, A., Cusack, M. and Reche, C.: Intense winter atmospheric pollution
694 episodes affecting the Western Mediterranean., Sci. Total Environ., 408(8), 1951–9,
695 doi:10.1016/j.scitotenv.2010.01.052, 2010.
- 696 Pey, J., Querol, X., Alastuey, A., Forastiere, F., and Stafoggia, M.: African dust outbreaks over the Mediterranean
697 Basin during 2001–2011: PM10 concentrations, phenomenology and trends, and its relation with synoptic and
698 mesoscale meteorology, Atmos. Chem. Phys., 13, 1395-1410, doi:10.5194/acp-13-1395-2013, 2013.
- 699 Querol, X., Viana, M., Alastuey, A., Amato, F., Moreno, T., Castillo, S., Pey, J., de la Rosa, J., Artiñano, B.,
700 Salvador, P., García Dos Santos, S., Fernández-Patier, R., Moreno-Grau, S., Negral, L., Minguillón, M.C., Monfort,
701 E., Gil, J.I., Inza, A., Ortega, L.A., Santamaría, J.M., Zabalza, J.: Source origin of trace elements in PM from
702 regional background, urban and industrial sites of Spain, Atmos. Environ., 41, 7219-7231, 2007.
- 703 Querol, X., Alastuey, A., Moreno, T., Viana, M.M., Castillo, S., Pey, J., Rodríguez, S., Artiñano, B., Salvador, P.,
704 Sánchez, M., Garcia Dos Santos, S., Herce Garraleta, M.D., Fernandez-Patier, R., Moreno-Grau, S., Negral, L.,
705 Minguillón, M.C., Monfort, E., Sanz, M.J., Palomo-Marín, R., Pinilla-Gil, E., Cuevas, E., de la Rosa, J., Sánchez de la

- 706 Campa, A.: *Spatial and temporal variations in airborne particulate matter (PM10 and PM2.5) across Spain 1999–*
707 *Atmos. Environ.*, 42, 3694–3979, 2008.
- 708 Querol, X., M. Viana, T. Moreno, A. Alastuey, J. Pey, F. Amato, M. Pandolfi, et al., *Scientific bases for a National*
709 *Air Quality Plan* (in Spanish), Colección Informes CSIC, 978-84-00-09475-1, 3, 2012.
- 710 Querol, X., , Alastuey, A., Pandolfi, M., Reche, C., Pérez, N., Minguillón, M.C., Moreno, T., Viana, M., Escudero,
711 M., Orio, A., Pallarés, M., Reina, F.: *2001–2012 trends on air quality in Spain*, *Sci. Total Environ.*, 490, 957–969,
712 doi:10.1016/j.scitotenv.2014.05.074, 2014
- 713 Salmi, T., Maata, A., Antilla, P., Ruoho-Airola, T., Amnell, T.: Detecting trends of annual values of atmospheric
714 pollutants by the Mann Kendall test and Sen's slope estimates – the Excel template application Makesens,
715 Finnish Meteorological Institute, Helsinki, Finland, 35 pp, 2002.
- 716 Salvador P., Artíñano B., Viana M., Alastuey A., Querol X.: *Evaluation of the changes in the Madrid metropolitan*
717 *area influencing air quality: analysis of 1999–2008 temporal trend of Particulate Matter*, *Atmos. Environ.*, 57,
718 175–185, 2012.
- 719
- 720 Sen, P.K., *Estimates of regression coefficient based on Kendall's tau*, *J. Am. Stat. Assoc.*, 63, 1379–1389, 1968
- 721 Shatalov V., Ilyin I., Gusev A., Rozovskaya O., Travnikov O.: *Heavy Metals and Persistent Organic Pollutants:*
722 *development of multi-scale modeling and trend analysis methodology*. EMEP/MSC-E Technical report 1/2015,
723 2015.
- 724 Smith, D.M.: *Computing single parameter transformations*, *Communications in Statistics - Simulation and*
725 *Computation*, 32, 605–618, 2002.
- 726 Theil, H.: *A rank invariant method of linear and polynomial regression analysis, I, II, III*, Proceedings of the
727 Koninklijke Nederlandse Akademie Wetenschappen, SeriesA — Mathematical Sciences, 386–392, 521–525,
728 1397–1412, 1950.
- 729 UNECE: Towards Cleaner Air. Scientific Assessment Report. EMEP Steering Body and Working Group on Effects
730 of the Convention on Long-Range Transboundary Air Pollution, Oslo. xx+50pp, Eds. Maas, R., P. Grennfelt,
731 www.unece.org/environmental-policy/conventions/envlratapwelcome/publications.html, 2016.
- 732 Williams, M.L., D. Carslaw, *New directions: science and policy — out of step on NO_x and NO₂?*, *Atmos. Environ.*,
733 45, 3911–3912, 2011.
- 734
- 735

736 **Table 1:** Trends of different PM mass fractions from gravimetry (grav) and optical (OPC) measurements at BCN (bold italic) and MSY
 737 (2004-2014). TR (%) = Total Reduction; RC (%) = Residual Component. Significance of the trends following the Mann-Kendall test: *** (p-
 738 value < 0.001), ** (p-value < 0.01), * (p-value < 0.05), + (p-value < 0.1).

PM _x	PM _x		Mann-Kendall fit			
	Fraction	Conc. 2004 (μgm^{-3})	Conc. 2014 (μgm^{-3})	p- value	Trend [$\mu\text{gm}^{-3}/\text{yr}$]	TR [%]
PM ₁₀ (grav.)	41.1	19.2	***	-2.83	59.2	8.5
	19.2	13.9		-0.17	10.5	17.6
PM _{2.5} (grav.)	31.6	13.2	***	-2.03	60.1	7.9
	16.2	9.8	+	-0.33	25.6	17.3
PM ₁₀ (OPC)	39.1	19.8	***	-2.20	50.4	10.0
	18.6	12.3		-0.13	7.8	16.9
PM _{2.5} (OPC)	27.1	12.9	**	-1.55	49.6	9.8
	16.5	9.3	+	-0.26	21.2	17.5

739

740

741

742

743

744

745

746

747

748

749

750

751

752

753

754

755

756

757
758
759
760
761

Table 2: Mann-Kendall and Multi-exponential trends of different chemical species in PM₁₀ at BCN (bold italic) and MSY. Type of trend: linear (L), single-exponential (SE), double exponential (DE); a (μgm^{-3}) and τ (yr) are the constants and the characteristic times, respectively, of the exponential data fittings; NL (%) = Non-Linearity; TR (%) = Total Reduction; RC (%) = Residual Component; ns = not statistically significant; ni = not included. Significance of the trends: *** (p-value < 0.001), ** (p-value < 0.01), * (p-value < 0.05), + (p-value < 0.1).

Species	PM ₁₀ (BCN;MSY)		Fit type	NL (%)	p-value	Mann-Kendall fit	Multi-exponential fit			TR (%)	RC (%)
	Concentration 2004 (μgm^{-3})	Concentration 2014 (μgm^{-3})				Trend [$\mu\text{gm}^{-3}/\text{yr}$]	a (μgm^{-3})	τ (yr)	Trend [$\mu\text{gm}^{-3}/\text{yr}$]		
Pb	0.02685	0.00694	SE	27	***		0.03246	6.12	-0.00222	80	17
	0.00481	0.00190	SE	11	**		0.00553	10.22	-0.00031	62	13
Cd	0.00043	0.00015	SE	19	***		0.00048	7.59	-3.10E-5	73	17
	0.00017	0.00006	SE	18	**		0.00018	7.92	-1.12E-5	72	16
As	0.00094	0.00036	SE	14	***		0.00118	9.11	-7.07E-5	67	11
	0.00029	0.00017	L	<10	***	-1.29E-5				50	9
V	0.01116	0.00454	SE	12	**		0.01502	10.04	-0.00086	63	17
	0.00328	0.00175	L	<10	**	-0.00022				59	15
Ni	0.00531	0.00284	SE	11	***		0.00678	10.61	-0.00037	61	16
	0.00155	0.00100	L	<10	**	-7.10E-5				43	20
Sn	<i>ni</i>	<i>ni</i>									
	0.00127	0.00057	L	<10	*	-3.65E-5				39	16
Cu	<i>ni</i>	<i>ni</i>									
	0.00420	0.00216	L	<10	*	-0.00014				36	20
Sb	<i>ni</i>	<i>ni</i>									
	0.00058	0.00025	SE	11	**		0.00064	10.46	-3.57E-5	62	13
SO ₄ ²⁻	5.74436	2.28596	SE	12	***		6.56033	9.81	-0.37868	64	12
	2.84849	1.67712	L	<10	**	-0.11836				42	18
NO ₃ ⁻	5.07816	1.72401	SE	12	**		6.49890	9.83	-0.37484	64	15
	1.80724	0.67419	L	<10	**	-0.10593				54	13
NH ₄ ⁺	1.92062	0.57008	SE	12	***		1.90645	9.64	-0.11095	65	14
	1.14268	0.40135	SE	13	*		1.28868	9.26	-0.07640	66	22
Al ₂ O ₃	<i>ni</i>	<i>ni</i>									
	0.72357	0.46382	L	<10	*	-0.02383				34	18
Ca	<i>ni</i>	<i>ni</i>									
	0.42703	0.28279	L	<10	*	-0.01638				38	17
Fe	<i>ni</i>	<i>ni</i>									
	0.22371	0.14895	L	<10	+	-0.00593				6	44
Na	1.02188	0.77408	L	<10	*	-0.03943				34	12
					ns						

762
763
764
765
766
767
768
769
770
771

772
773
774
775
776

Table 3: Mann-Kendall and Multi-exponential trends of different chemical species in PM_{2.5} at BCN (bold italic) and MSY. Type of trend: linear (L), single-exponential (SE), double exponential (DE); a (μgm^{-3}) and τ (yr) are the constants and the characteristic times, respectively, of the exponential data fittings; NL (%) = Non-Linearity; TR (%) = Total Reduction; RC (%) = Residual Component; ns = not statistically significant; ni = not included. Significance of the trends: *** (p-value < 0.001), ** (p-value < 0.01), * (p-value < 0.05), + (p-value < 0.1).

	PM _{2.5} (BCN;MSY)		Fit type	NL (%)	p-value	Mann-Kendall fit	Multi-exponential fit			TR (%)	RC (%)
	Concentration 2004 (μgm^{-3})	Concentration 2014 (μgm^{-3})				Trend [$\mu\text{gm}^{-3}/\text{yr}$]	a (μgm^{-3})	τ (yr)	Trend [$\mu\text{gm}^{-3}/\text{yr}$]		
Pb	0.02117	0.00500	SE	27	***		0.02390	6.24	-0.00163	80	13
	0.00642	0.00149	SE	28	***		0.00716	6.08	-0.00049	81	18
Cd	0.00041	0.00011	SE	23	***		0.00047	6.81	-3.11E-5	77	13
	0.00020	0.00005	SE	23	***		0.00020	6.77	-1.35E-5	77	18
As	0.00069	0.00027	SE	14	***		0.00091	9.00	-5.43E-5	67	11
	0.00029	0.00013	SE	15	**		0.00033	8.56	-2.04E-5	69	19
V	0.00823	0.00368	SE	11	**		0.01121	11.13	-0.00061	59	16
	0.00271	0.00130	L	<10	**	-0.00017				64	24
Ni	0.00402	0.00185	SE	10	**		0.00498	11.23	-0.00027	59	15
	0.00189	0.00080	SE	13	**		0.00205	9.36	-0.00012	42	21
Sn	<i>ni</i>	<i>ni</i>									
	0.00157	0.00043	L	<10	***	-0.00084				61	12
Cu	<i>ni</i>	<i>ni</i>									
	0.00394	0.00113	SE	14	**		0.00426	8.99	-0.00026	67	13
Sb	<i>ni</i>	<i>ni</i>									
	0.00053	0.00015	DE	48	**		0.00069 1.3E-6	4.52 -2.50	-3.86E-5	70	16
SO_4^{2-}	4.86564	1.92388	SE	12	***		5.64582	9.69	-0.32778	64	9
	2.98922	1.43381	L	<10	**	-0.16222				54	15
NO_3^-	3.45513	0.86002	SE	19	***		4.14459	7.61	-0.26753	73	16
	1.66095	0.29452	SE	30	***		1.96014	5.81	-0.13550	82	21
NH_4^+	2.19735	0.68393	SE	11	***		2.27813	10.53	-0.12701	61	15
	1.39366	0.48049	SE	18	**		1.62588	7.94	-0.10266	72	14
Al_2O_3	<i>ni</i>	<i>ni</i>									
	0.30245	0.10153	SE	13	*		0.26678	9.36	-0.01574	66	35
Ca	<i>ni</i>	<i>ni</i>									
	0.11478	0.06540	L	<10	+	-0.00494				50	33
Fe	<i>ni</i>	<i>ni</i>									
	0.09679	0.03716	L	<10	*	-0.00504				61	31
Na	0.27476	0.17863	L	<10	+	-0.01247				41	15
	0.13091	0.07252	L	<10	*	-0.00584				45	18

777

778

779

780

781

782

783

784

785

786 **Table 4:** Mann-Kendall and Multi-exponential trends of source contributions in PM₁₀ from PMF at BCN (bold italic) and MSY. Type: linear
 787 (L), single-exponential (SE), double exponential (DE); a (μgm^{-3}) and τ (yr) are the constants and the characteristic times, respectively, of
 788 the exponential data fittings; NL (%) = Non-Linearity; TR (%) = Total Reduction; RC (%) = Residual Component; ni = not included .
 789 Significance of the trends following the Mann-Kendall test: *** (p-value < 0.001), ** (p-value < 0.01), * (p-value < 0.05), + (p-value < 0.1).

Source	PM ₁₀ (BCN;MSY)		Fit type	NL (%)	p-value	Mann-Kendall fit	Multi-exponential fit			TR (%)	RC (%)
	Contribution 2004 (μgm^{-3})	Contribution 2014 (μgm^{-3})				Trend [$\mu\text{gm}^{-3}/\text{yr}$]	a (μgm^{-3})	τ (yr)	Trend [$\mu\text{gm}^{-3}/\text{yr}$]		
<i>Secondary sulfate</i>	10.27	3.38	<i>DE</i>	45	**		12.33 3.82	1.65 105.80	-0.71	67	16
	6.57	3.07	SE	12	**		5.99	13.22	-0.32	53	21
<i>Secondary nitrate</i>	6.99	1.96	<i>SE</i>	14	***		8.54	8.96	-0.51	67	13
	2.03	0.47	SE	15	**		2.44	8.59	-0.15	69	17
<i>V-Ni bearing</i>	4.23	1.84	<i>SE</i>	11	**		5.66	10.59	-0.32	61	19
	0.79	0.44	L	8	**	-0.07				64	25
<i>Industrial/Metallurgy (BCN)</i>	1.64	0.71	<i>SE</i>	21	***		1.76	9.56	-0.10	65	16
<i>Mineral</i>	<i>ni</i>	<i>ni</i>									
	3.46	2.32	L	5	+	-0.10				30	21
<i>Industrial/Traffic (MSY)</i>	2.08	1.01	L	7	**	-0.11				56	13

790

791

792

793

794

795

796

797

798

799

800

801

802

803

804

805

806

807 **Figure Captions:**

808 **Figure 1:** Location of the Barcelona (BCN) and Montseny (MSY) measuring stations. Red full circle highlights the location of the BCN
809 measuring station before 2009. Green full circle highlights the new location of the BCN (from 2009) and MSY measuring stations.

810 **Figure 2:** Mann-Kendall fit of PM_{2.5} trends at MSY station for the periods 2002-2010 (as in Cusack et al., 2012), 2004 – 2014 (this work),
811 and 2002 – 2014 (largest period available in the time of writing). Reported are: magnitude of the trends [$\mu\text{gm}^{-3}/\text{yr}$]; p-value; Total
812 Reduction (TR) and Residual Component (RC). Significance of the trends following the Mann-Kendall test: *** (p-value < 0.001), ** (p-
813 value < 0.01), * (p-value < 0.05), + (p-value < 0.1).

814 **Figure 3:** Mann-Kendall (MK) and Multi-exponential (ME) trends for chemical species at BCN in PM₁₀. Measured concentration (green
815 line); Multi-exponential trend (red line); Multi-exponential residuals (blue line); Mann-Kendall trend (black line); Mann-Kendall residuals
816 (grey line). Trend type: linear (L), single-exponential (SE), double exponential (DE).

817 **Figure 4:** Mann-Kendall (MK) and Multi-exponential (ME) trends for chemical species at MSY in PM₁₀. Measured concentration (green
818 line); Multi-exponential trend (red line); Multi-exponential residuals (blue line); Mann-Kendall trend (black line); Mann-Kendall residuals
819 (grey line). Trend type: linear (L), single-exponential (SE), double exponential (DE).

820 **Figure 5:** Source contributions from PMF model in PM₁₀ at Montseny (MSY) and Barcelona (BCN). Mean values during 2004-2014. Values
821 reported are: **Source; $\mu\text{g}/\text{m}^3$; %.**

822 **Figure 6:** Mann-Kendall and Multi-exponential trends for source contributions in PM₁₀ at BCN. Measured concentration (green line);
823 Multi-exponential trend (red line); Multi-exponential residuals (blue line); Mann-Kendall trend (black line); Mann-Kendall residuals (grey
824 line). Trend type: linear (L), single-exponential (SE), double exponential (DE). Highlighted with yellow colour the source contributions at
825 BCN from *Mineral, Traffic* and *Road/work resuspension* were excluded from the trend discussion.

826 **Figure 7:** Mann-Kendall and Multi-exponential trends for source contributions in PM₁₀ at MSY. Measured concentration (green line);
827 Multi-exponential trend (red line); Multi-exponential residuals (blue line); Mann-Kendall trend (black line); Mann-Kendall residuals (grey
828 line). Trend type: linear (L), single-exponential (SE), double exponential (DE).

829 **Figure 8:** Spanish national emission of SO₂ and NO_x (normalized to year 2004).

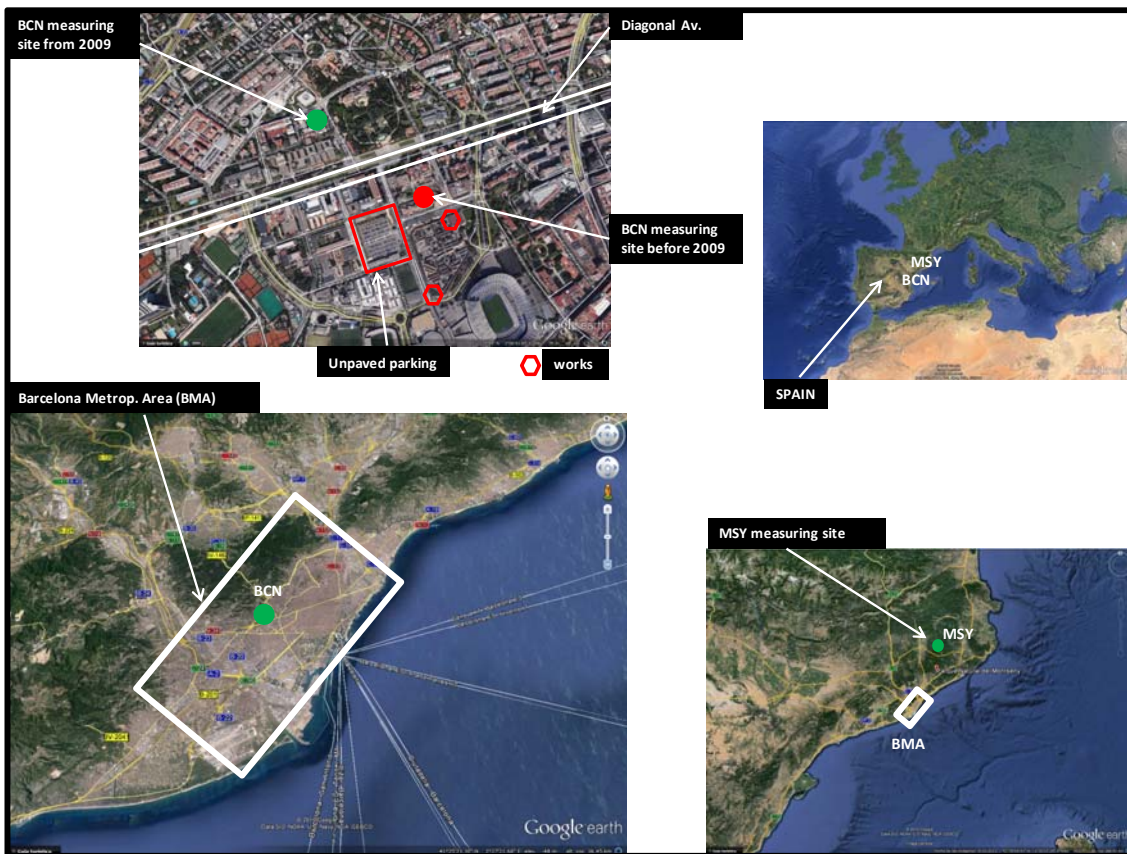
830 **Figure 9:** NASA OMI level 3 tropospheric NO₂ column plotted using the Giovanni online data system, developed and maintained by the
831 NASA GES DISC.

832 **Figure 10:** Annual (2004–2014) energy consumption for Spain (normalized to year 2004). Data from the Spanish Ministry of Industry
833 (MINETUR, 2013).

834

835

836



837

838 **Figure 1**

839

840

841

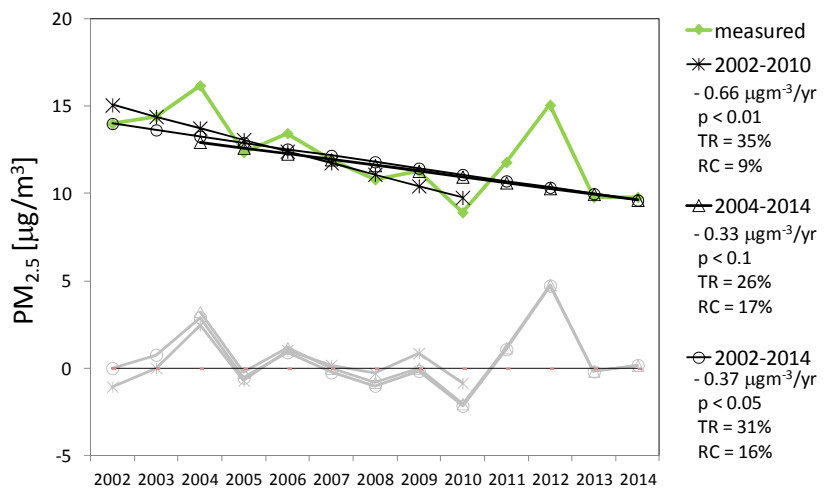
842

843

844

845

846



847

848 **Figure 2**

849

850

851

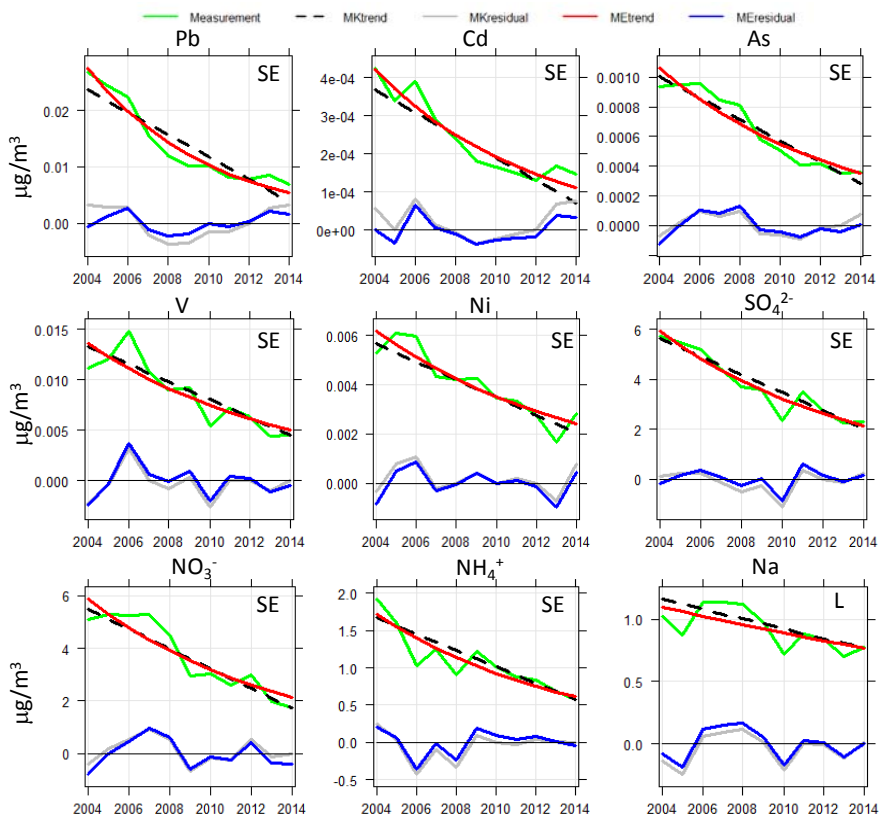
852

853

854

855

856



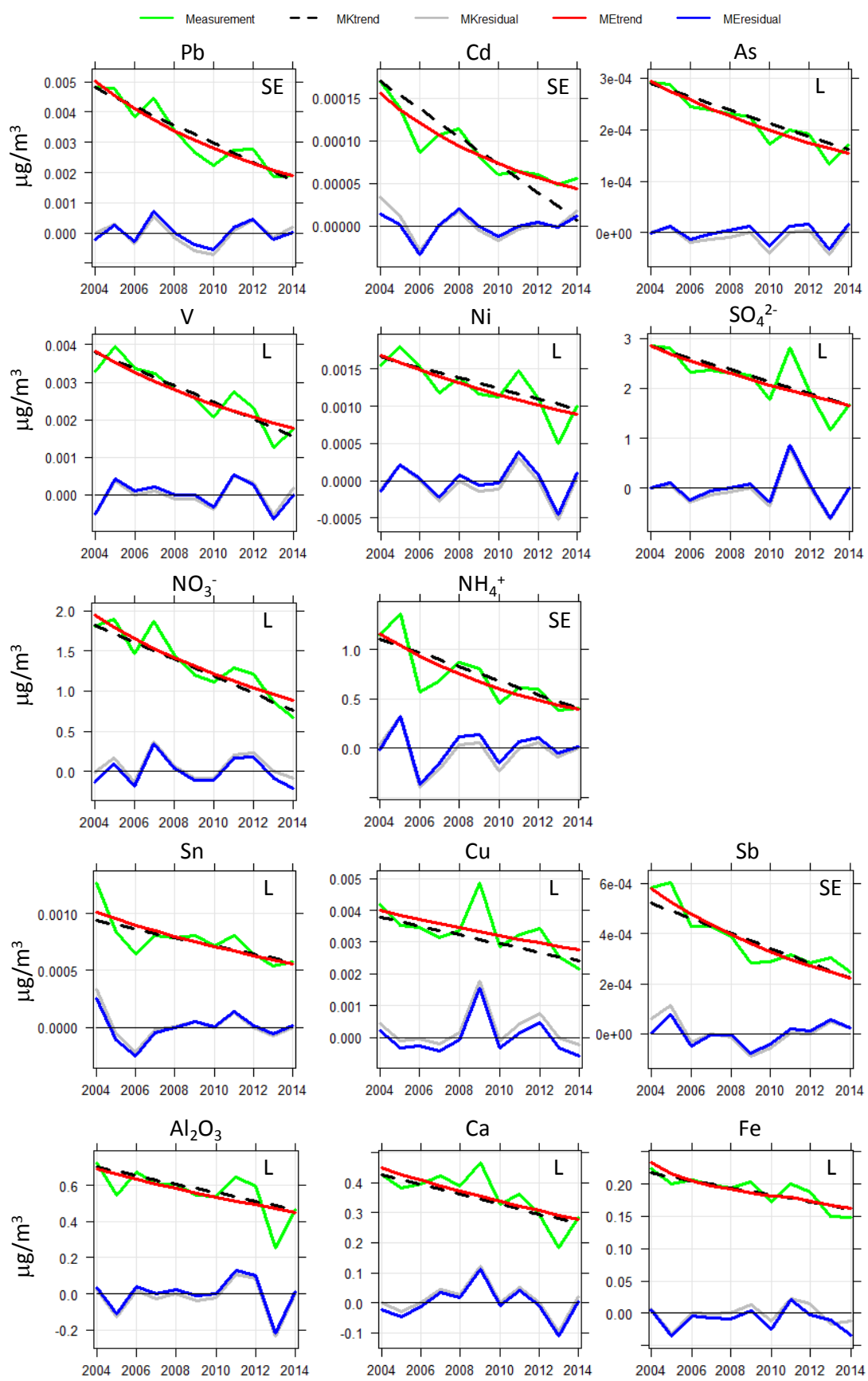
857

858 **Figure 3**

859

860

861



862

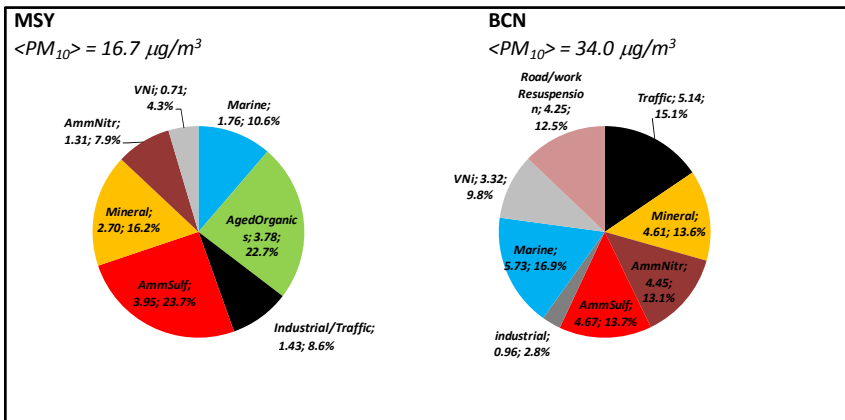
863

864 **Figure 4**

865

866

867



868

869 **Figure 5**

870

871

872

873

874

875

876

877

878

879

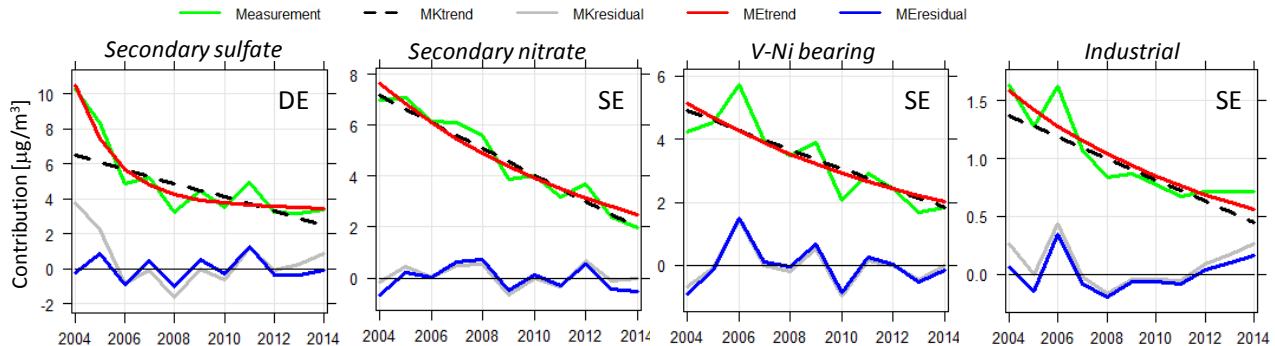
880

881

882

883

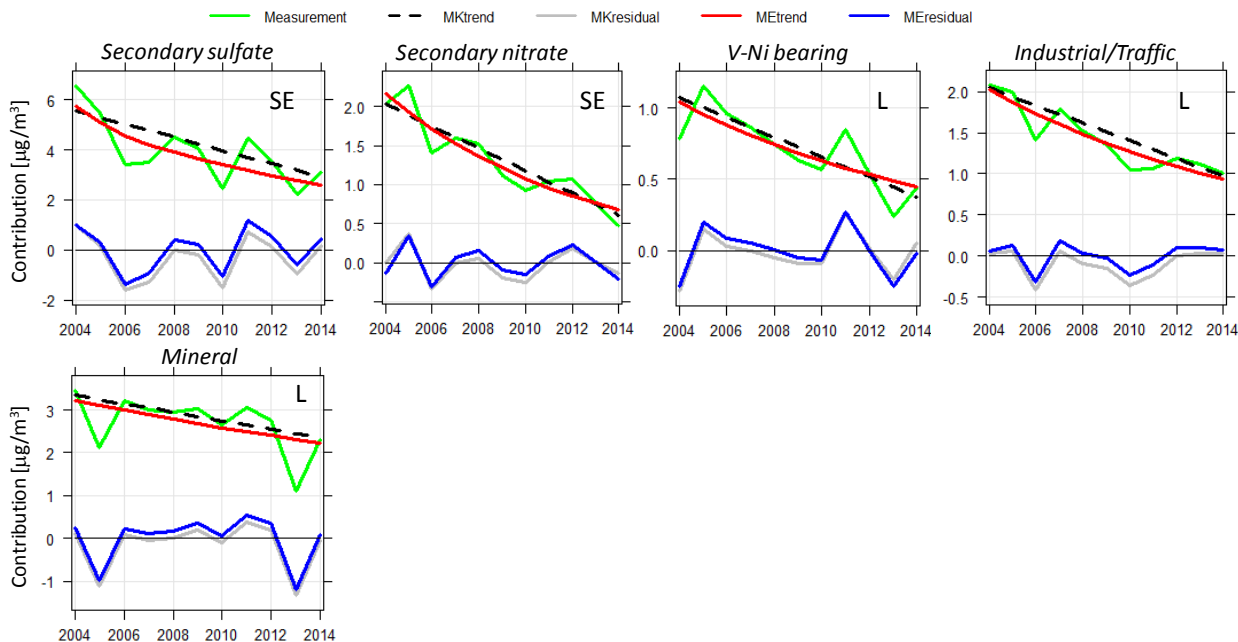
884



885

886 **Figure 6**

887



888

889 **Figure 7**

890

891

892

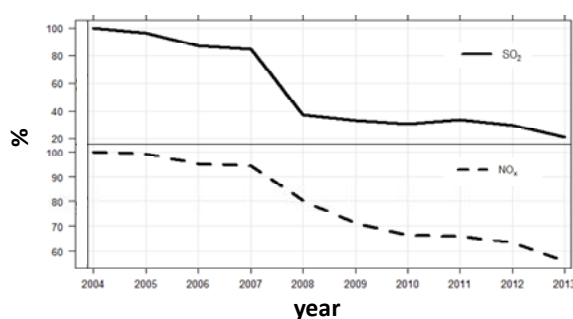
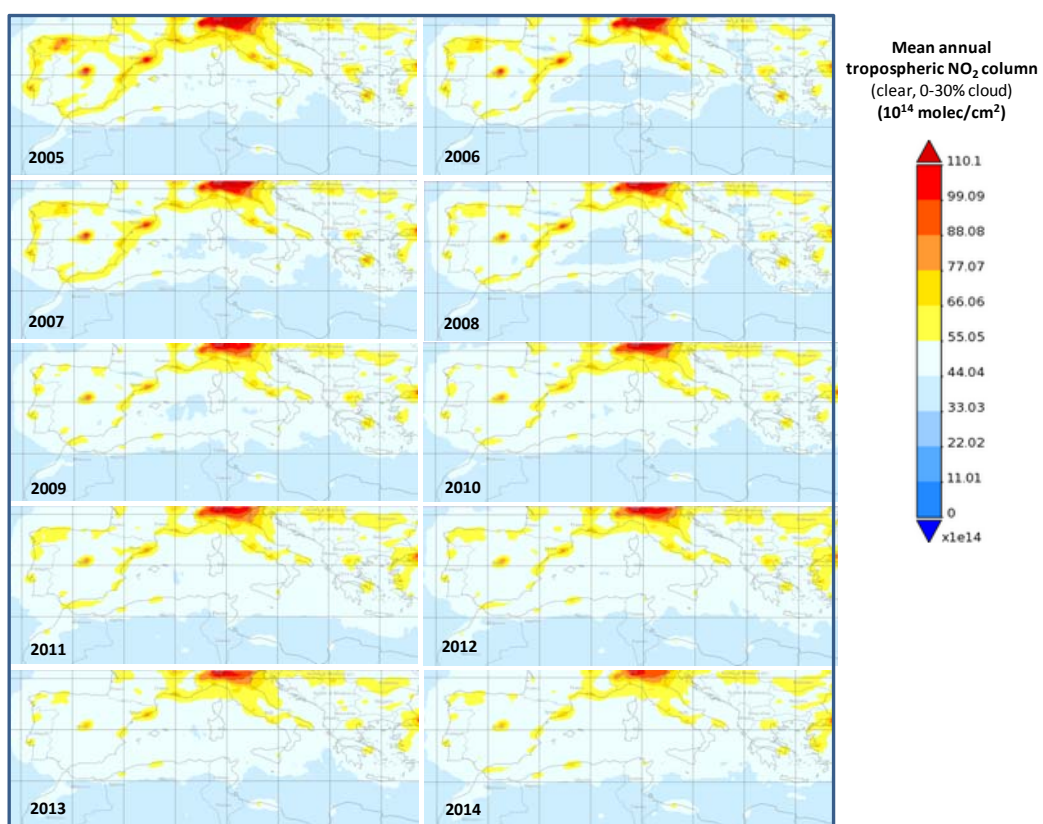
893

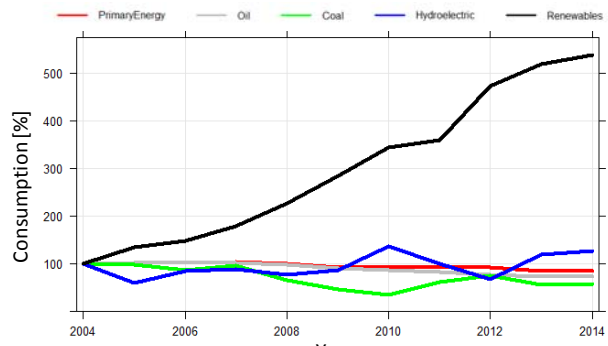
894

895

896

897

900 **Figure 8**904 **Figure 9**



909

910 **Figure 10**

911

912

913

914

915

916

917